Supporting Information

Microfluidic paper-based colorimetric device for visual and fluorescent detection of uric acid in practical samples

Arezoo Saadati [a,b], Fatemeh Farshchi [c], Mohammad Hasanzadeh [b,d*], Farzad Seidi [a**]

[a] Jiangsu Co-Innovation Center for Efficient Processing and Utilization of Forest Resources and International Innovation Center for Forest Chemicals and Materials, Nanjing Forestry University, Nanjing 210037, China.

[b] Pharmaceutical Analysis Research Center, Tabriz University of Medical Sciences, Tabriz, Iran.

[c] Drug Applied Research Center, Tabriz University of Medical Sciences, Tabriz, Iran.

[d] Nutrition Research Center, Tabriz University of Medical Sciences, Tabriz, Iran.

Corresponding Author

* (Mohammad Hasanzadeh) Pharmaceutical Analysis Research Center, Tabriz University of Medical Sciences, Tabriz, Iran.
E-mail address: (*) hasanzadehm@tbzmed.ac.ir

** (Farzad Seidi) Jiangsu Co-Innovation Center for Efficient Processing and Utilization of Forest Resources and International Innovation Center for Forest Chemicals and Materials, Nanjing Forestry University, Nanjing 210037, China E-mail address: (**) f_seidi@njfu.edu.cn.

(I)

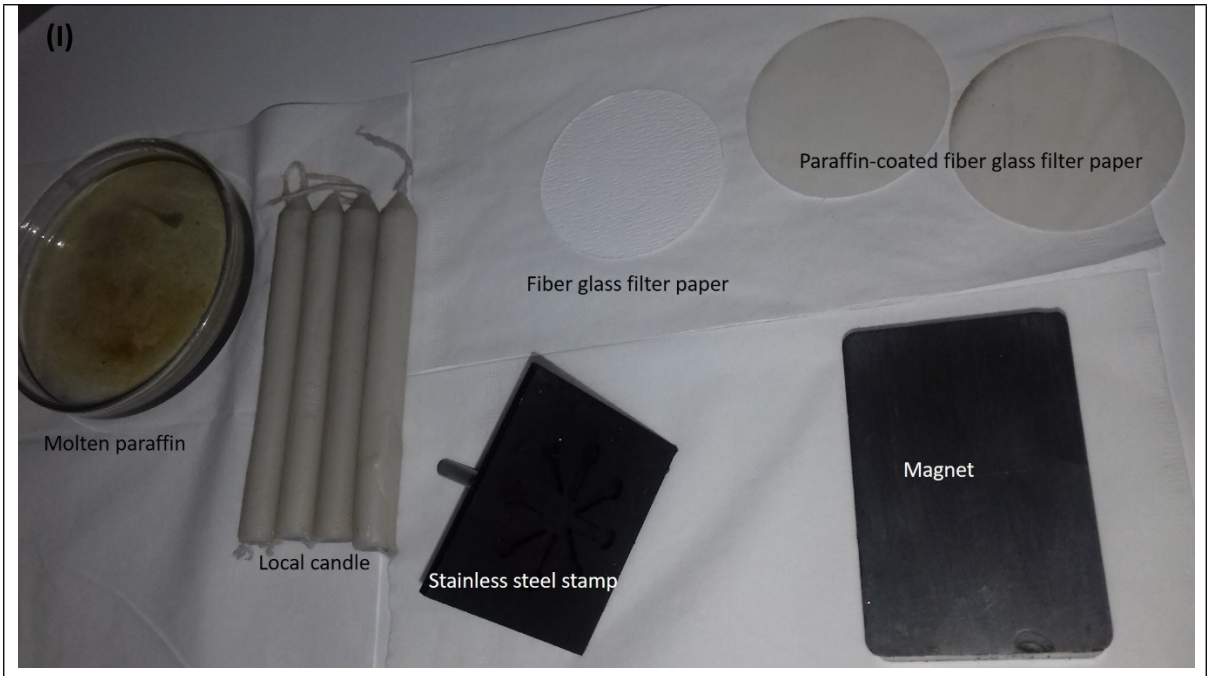
Paraffin-coated fiber glass filter paper
Fiber glass filter paper
Molten paraffin
Local candle
Stainless steel stamp
Magnet

(II)


A
B
C
D
n-paper
P-paper
POWER
90c

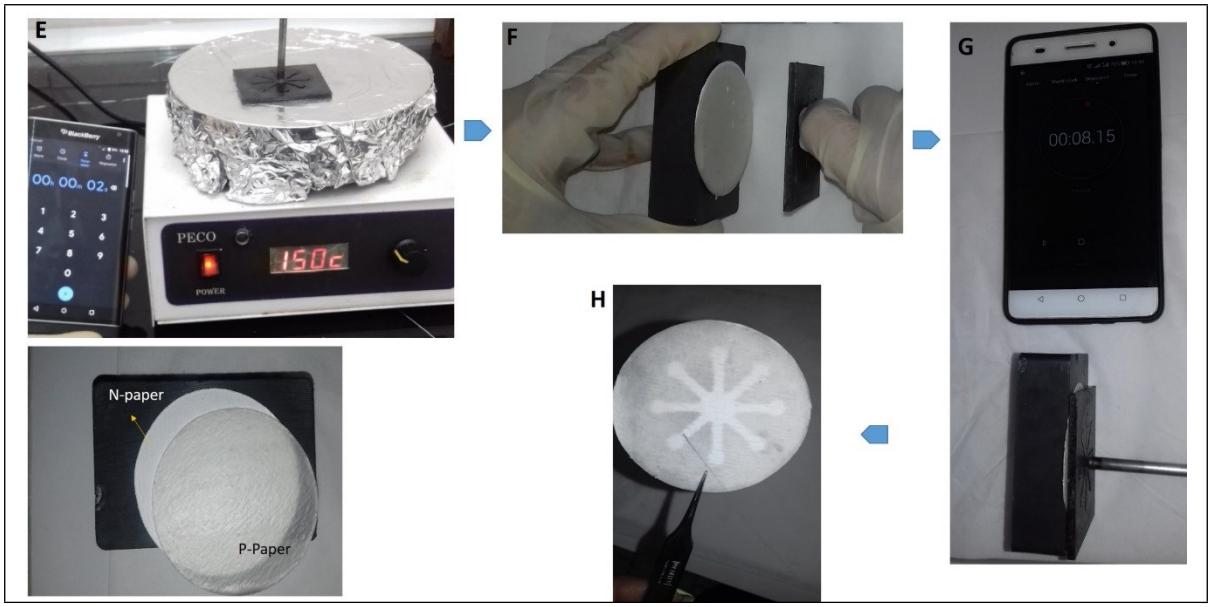
E
PECO
150c
F
G
00:08.15
H
N-paper
P-Paper

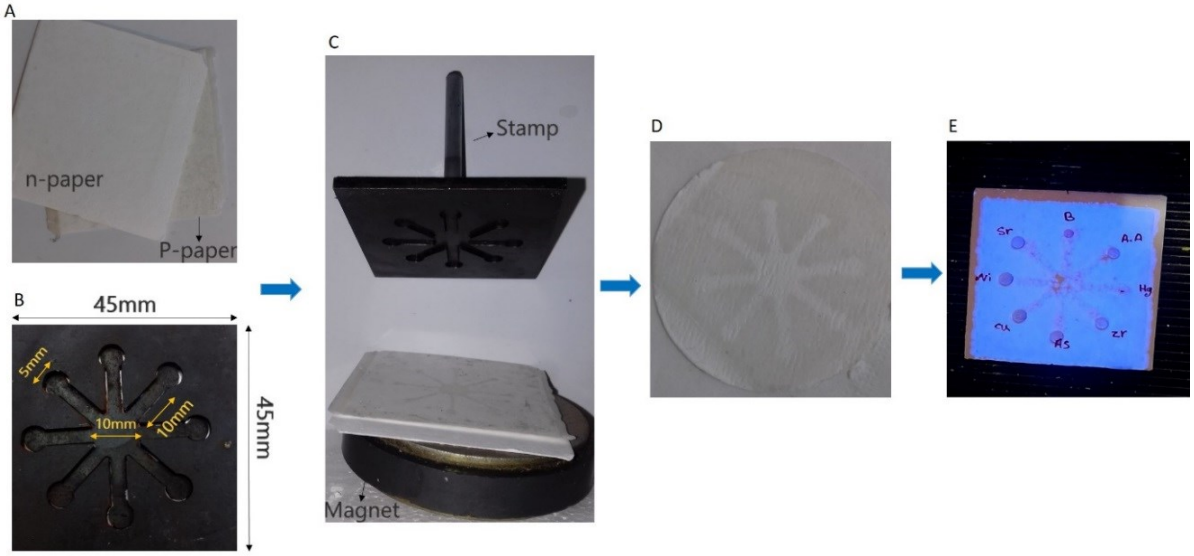
A
n-paper
P-paper
B
45mm
45mm
5mm
10mm
10mm
C
Stamp
Magnet
D
E

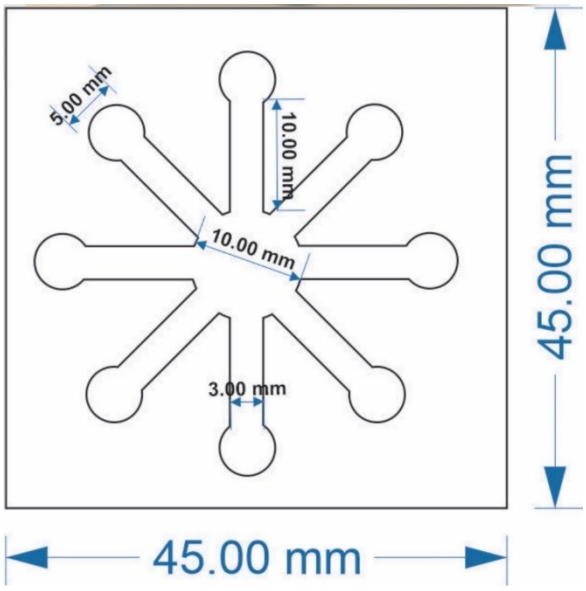
5.00 mm
10.00 mm
10.00 mm
3.00 mm
45.00 mm
45.00 mm

Scheme S1. Materials and equipment (I), and the process (II) of μPCD fabrication. Melt the paraffin of the local candles under 90℃, following by moothly placed the filter paper through it (A), and leaved it for 2s (B), afterwards, the filter paper was taken out (C) to prepare paraffinated paper (D). The locally machined steel stamp was heated on 150℃ for 2 s, and the p-paper was put on the n-paper (E), before stamping (F). The stamping step was performed during 8s (G) to prepare the proposed μPCD.

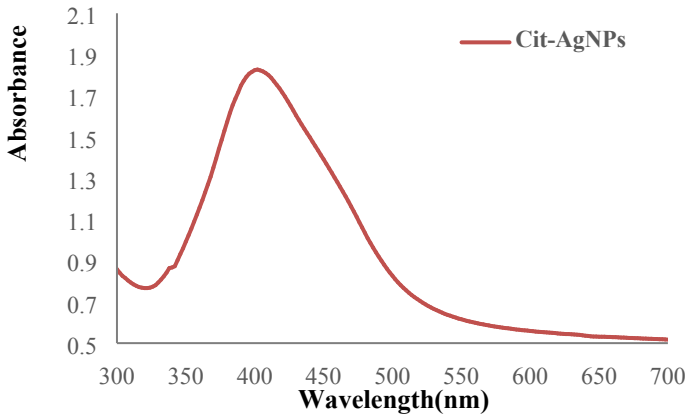
Absorbance
2.1
1.9
1.7
1.5
1.3
1.1
0.9
0.7
0.5
Cit-AgNPs
300
350
400
450
500
550
600
650
700
Wavelength(nm)

A

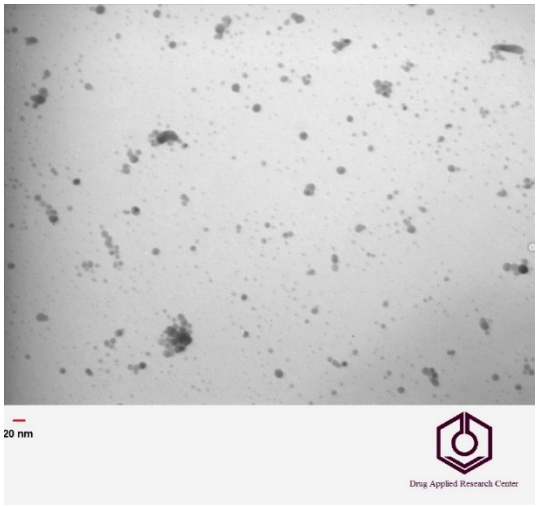
20 nm
Drug Applied Research Center

B

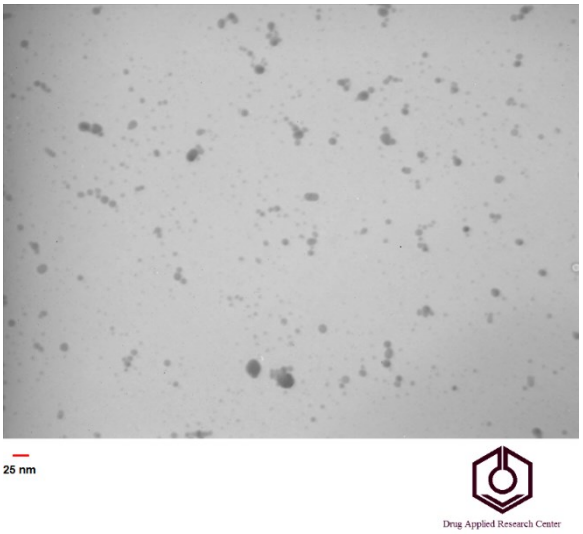
25 nm
Drug Applied Research Center

C

C

D

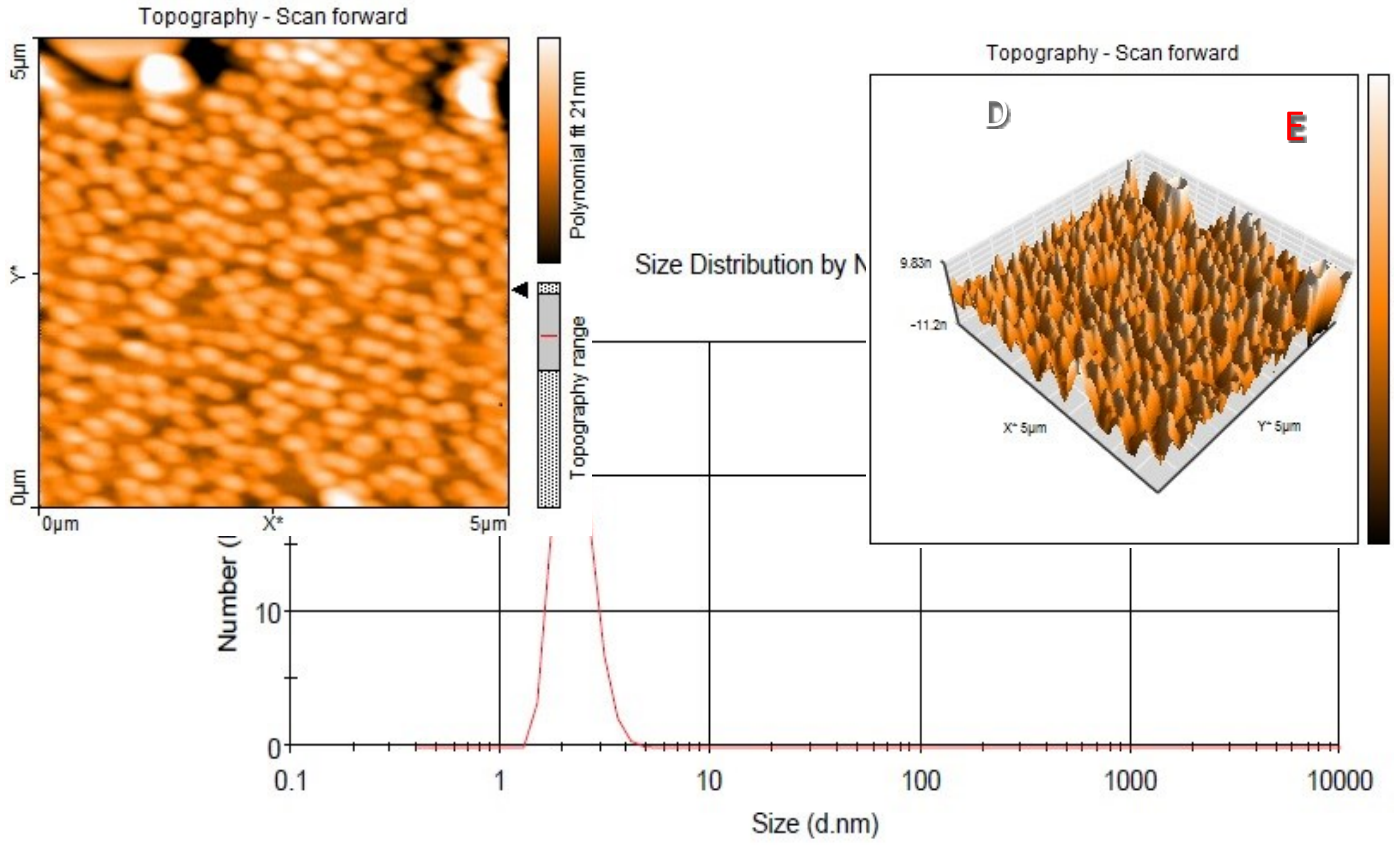
Topography - Scan forward
5µm
Y*
0µm
0µm
X*
5µm
Polynomial fit 21nm
Topography range
Size Distribution by N
Topography - Scan forward
D
E
9.83n
-11.2n
X* 5µm
Y* 5µm
Polynomial fit 21nm
Number (
10
0
0.1
1
10
100
1000
10000
Size (d.nm)

Figure S1. A) *UV-Vis absorbance spectrum of Ag citrate NPs. (B,C) TEM images of Ag citrate NPs in different magnification.*(D,E) *Topographic AFM images in 2D* ***(D)*** *and 3D* ***(E)*** *view of Ag citrate NPs. Dynamic light scattering (DLS) analysis of* ***F)*** *Ag citrate NPs,* ***G)*** *Ag citrate and uric acid mixture.*

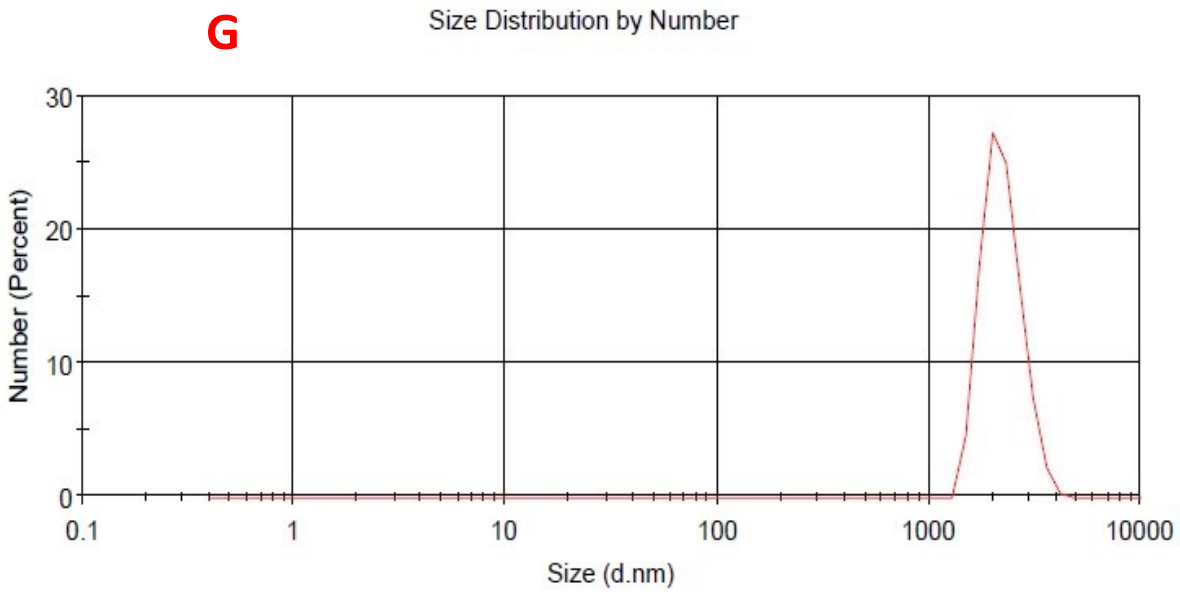

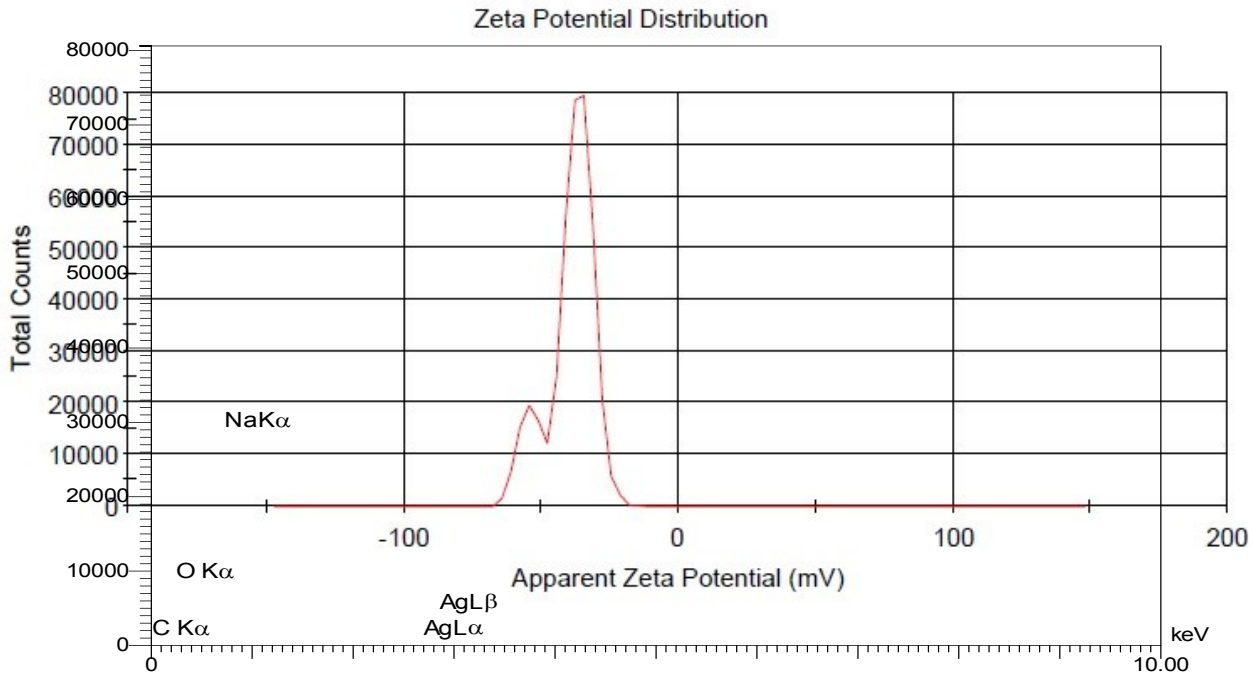

Figure S2. *Zeta potential of Ag citrate NPs.*

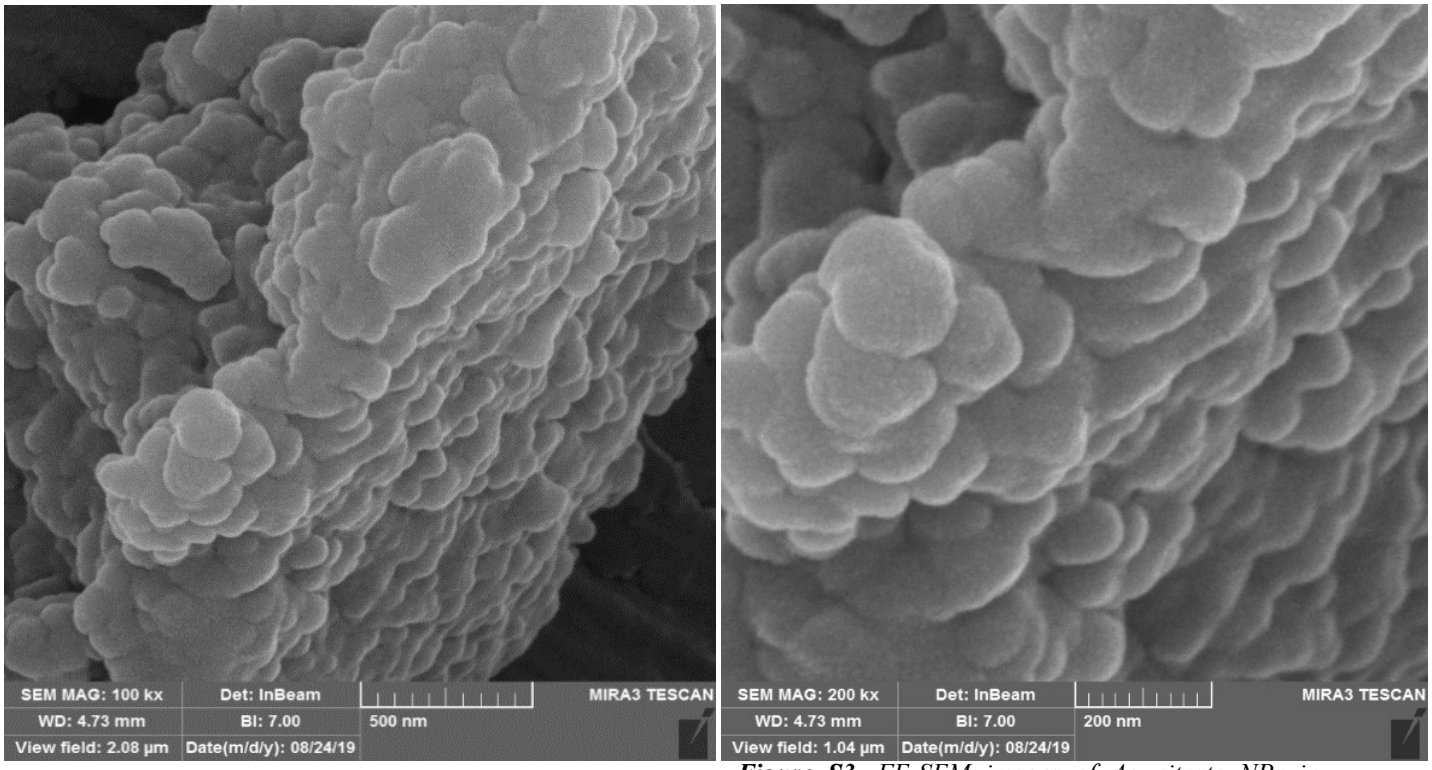

Figure S3. *FE-SEM images of Ag citrate NPs in different magnification.*

Figure S4. *EDS spectra of Ag citrate NPs.*

Elt	Int	W%
C	57.5	6.16
O	465.6	19.09
Na	2468.5	70.95
Ag	122.5	3.80
		100.00

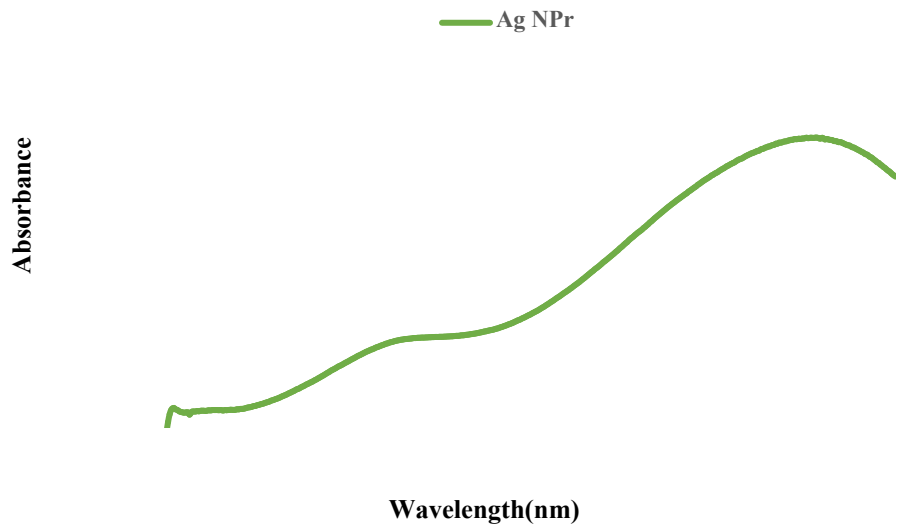

Figure S5. *UV-Vis absorbance spectrum of Ag NPrs.*

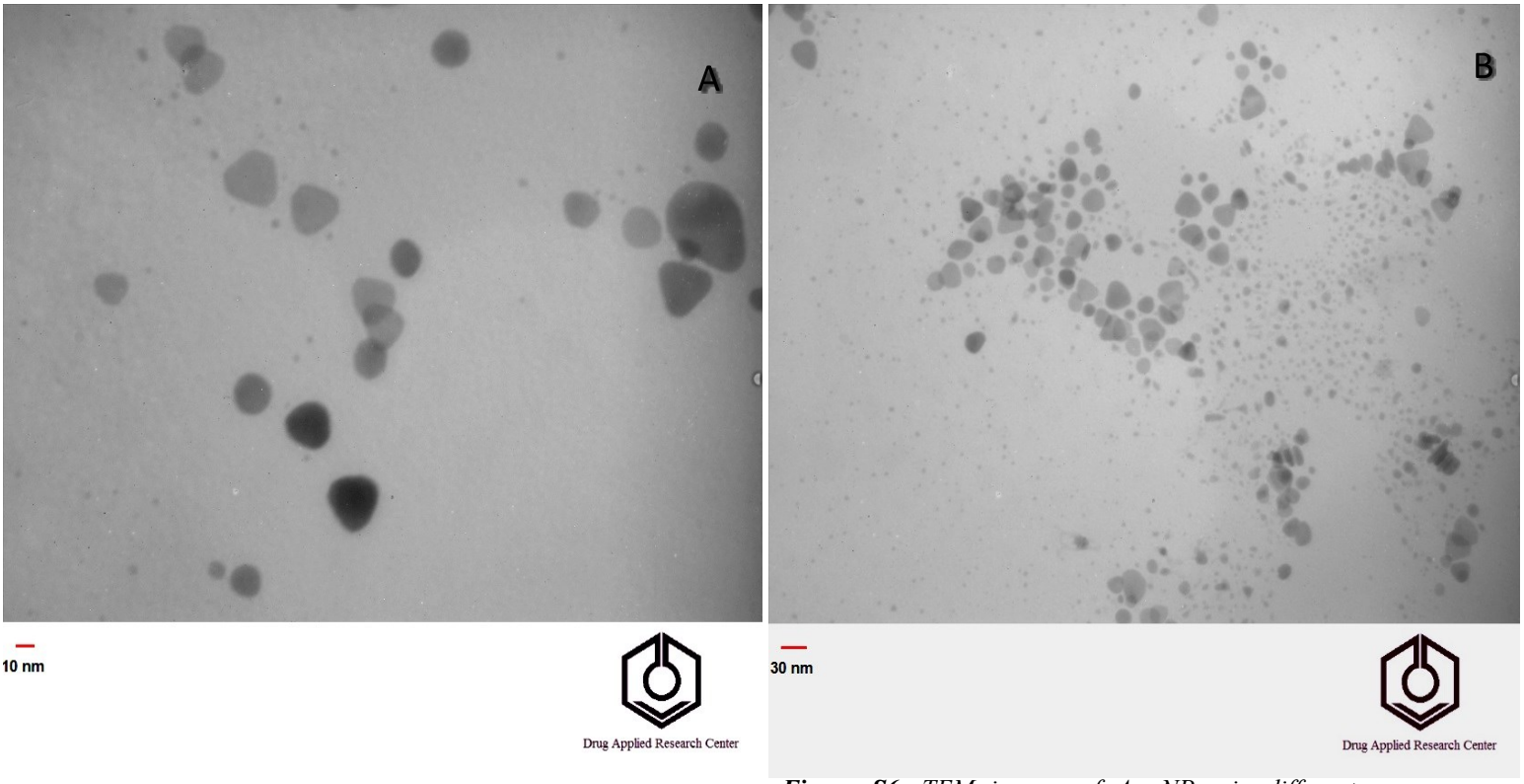

Figure S6. *TEM images of Ag NPrs in different magnification 10 nm (A) and 30 nm (B).*

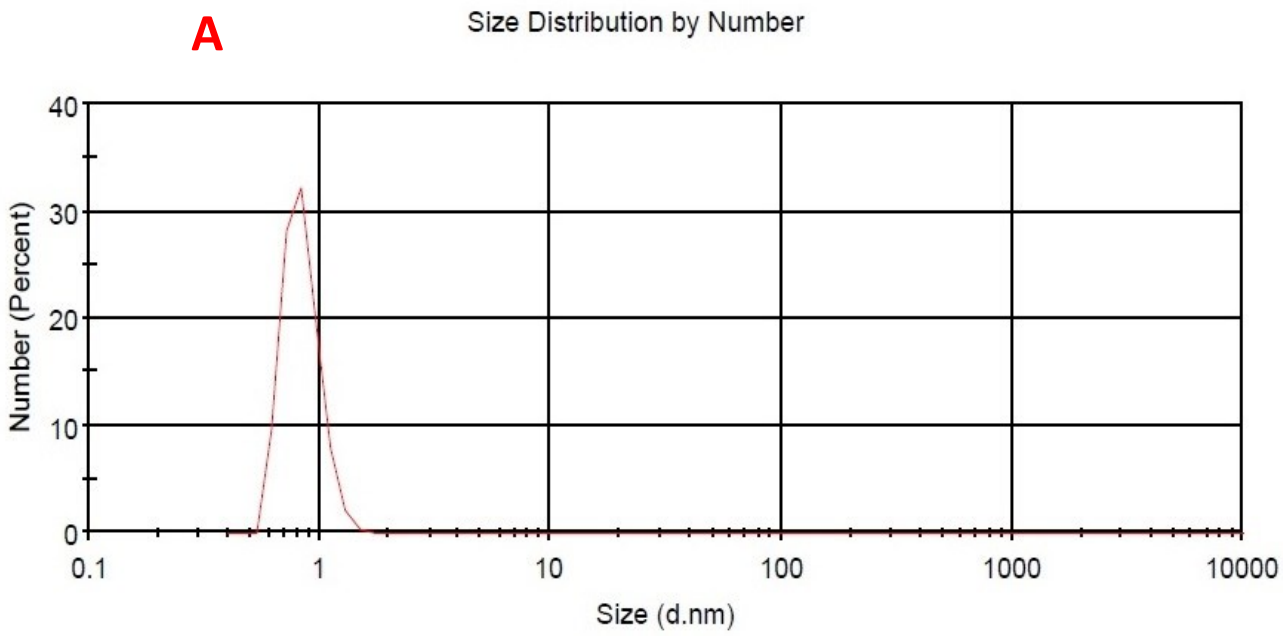

Figure S7. *Dynamic light scattering (DLS) analysis of* ***A)*** *Ag NPrs,* ***B)*** *Ag NPrs and uric acid mixture.*

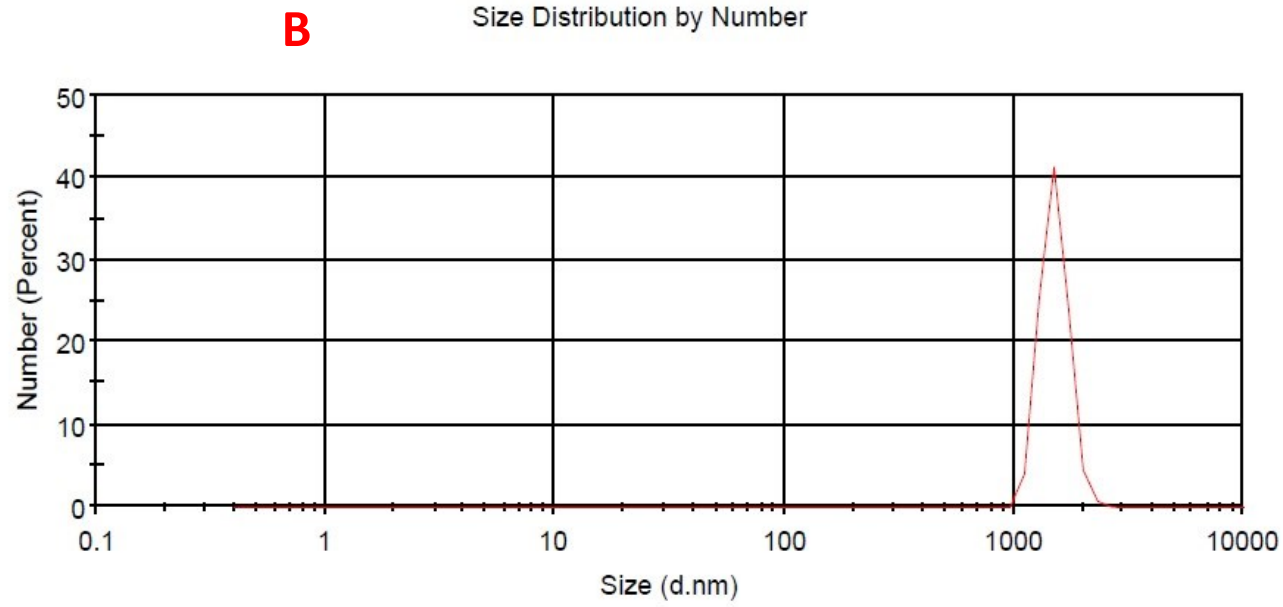

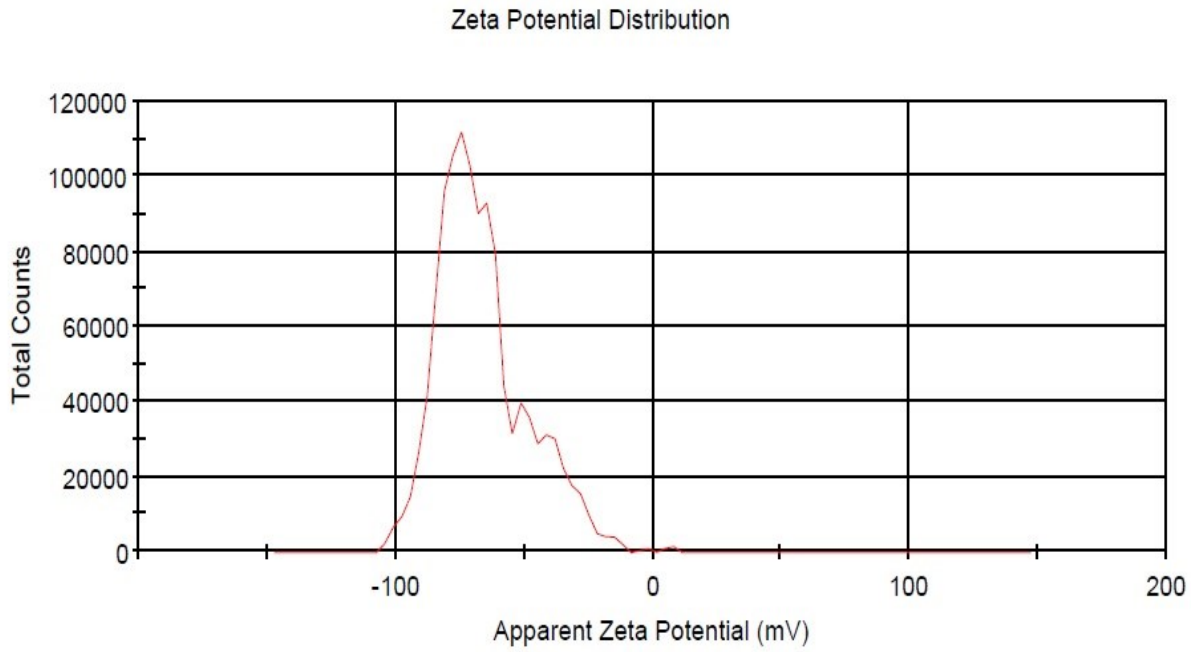

Figure S8. *Zeta potential of Ag NPrs.*

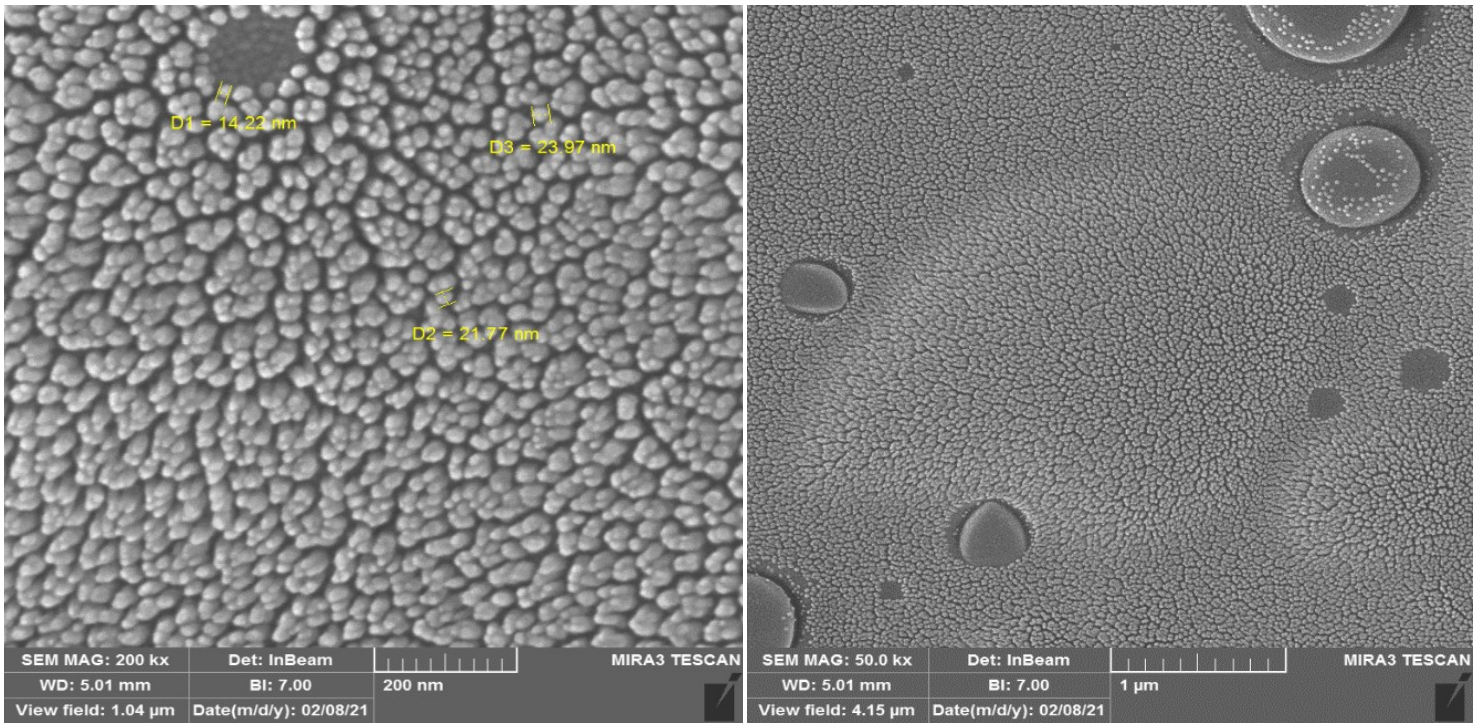

Figure S9. *FE-SEM images of Ag NPrs in different magnification.*

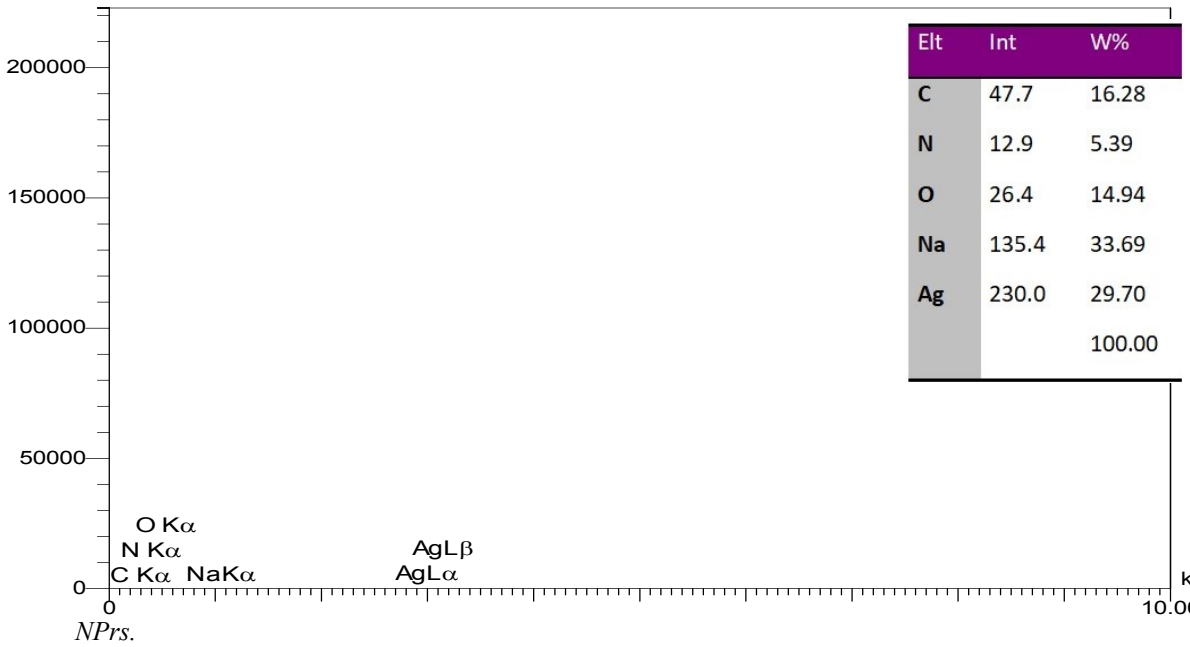

Elt	Int	W%
C	47.7	16.28
N	12.9	5.39
O	26.4	14.94
Na	135.4	33.69
Ag	230.0	29.70
		100.00

Figure S10. *EDS spectra of Ag NPrs.*

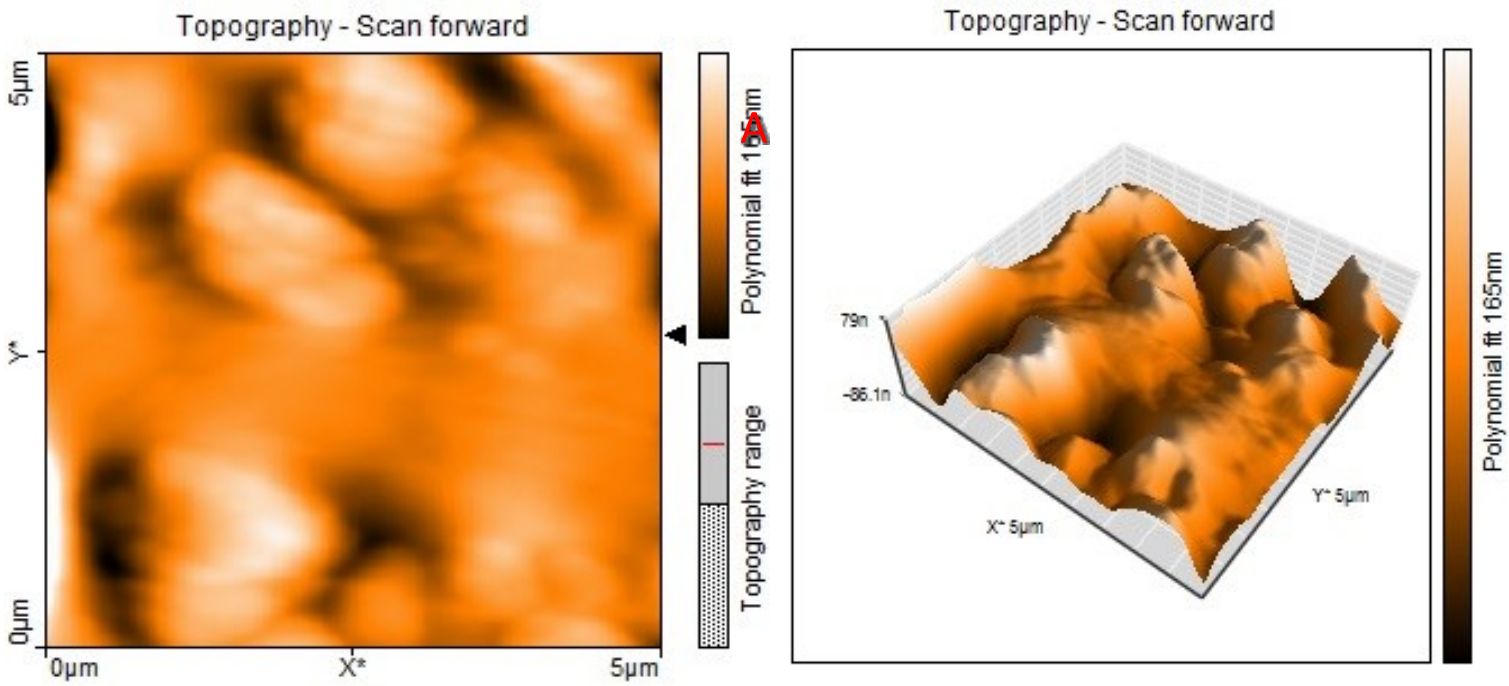

Figure S11. *Topographic AFM images of Ag NPrs in 2D* ***(A)*** *and 3D* ***(B)*** *view.*

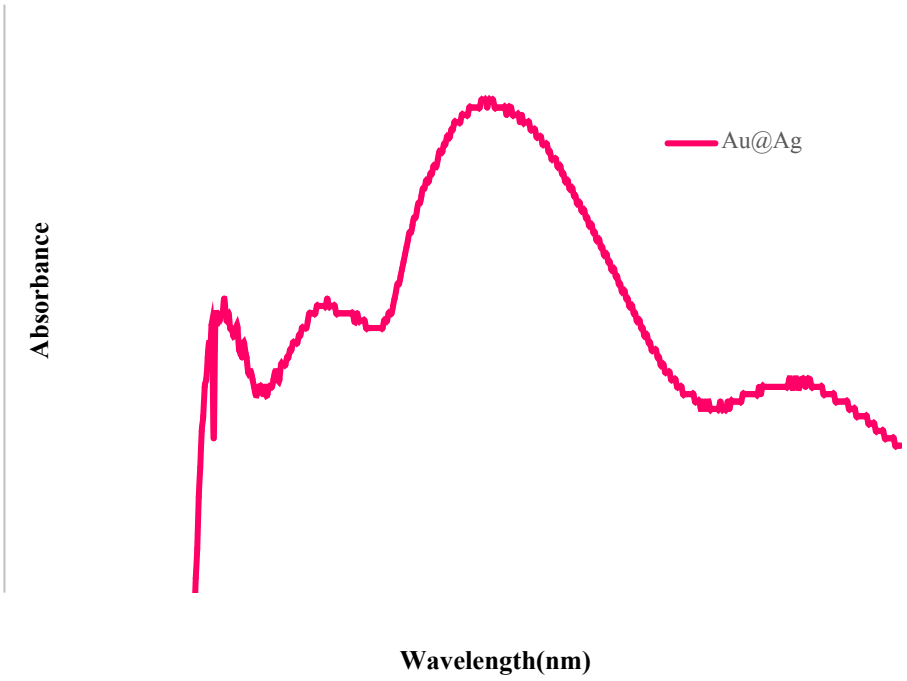

Figure S12. *UV-Vis absorbance spectrum of Au@Ag core-shell NPs.*

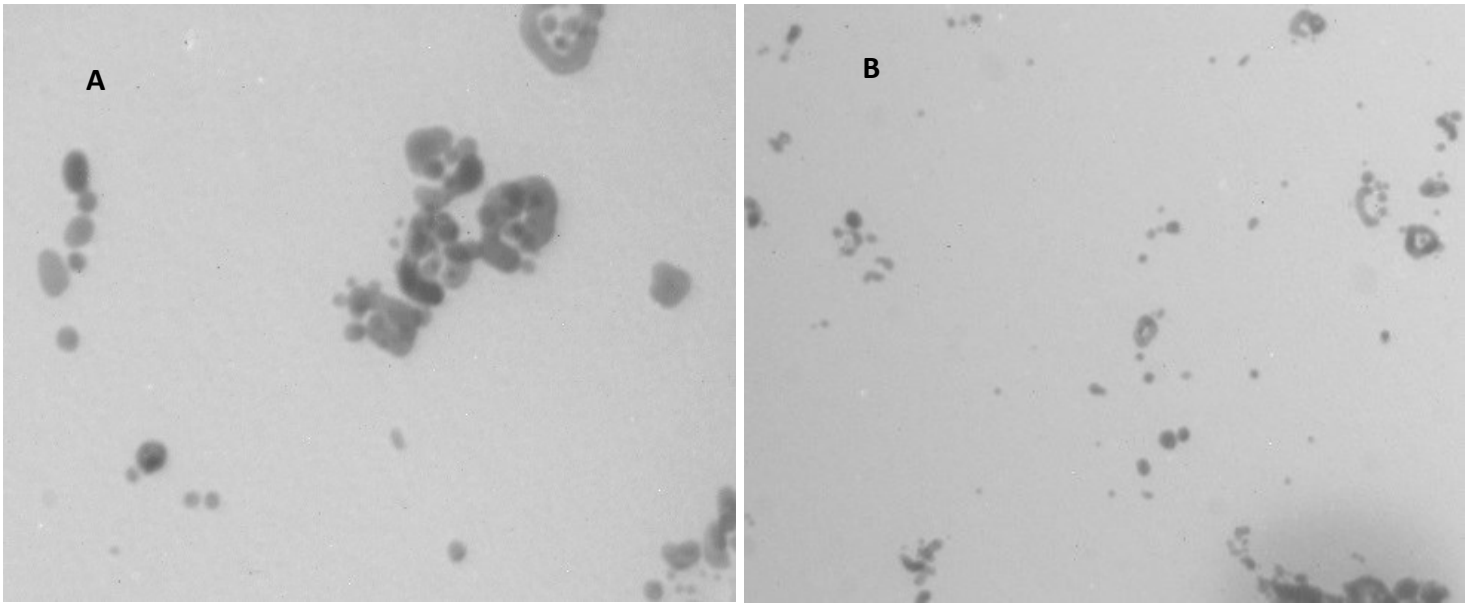

Figure S13. *TEM images of Au@Ag core-shell NPs in different magnification 15 nm (A) and 50 nm (B).*

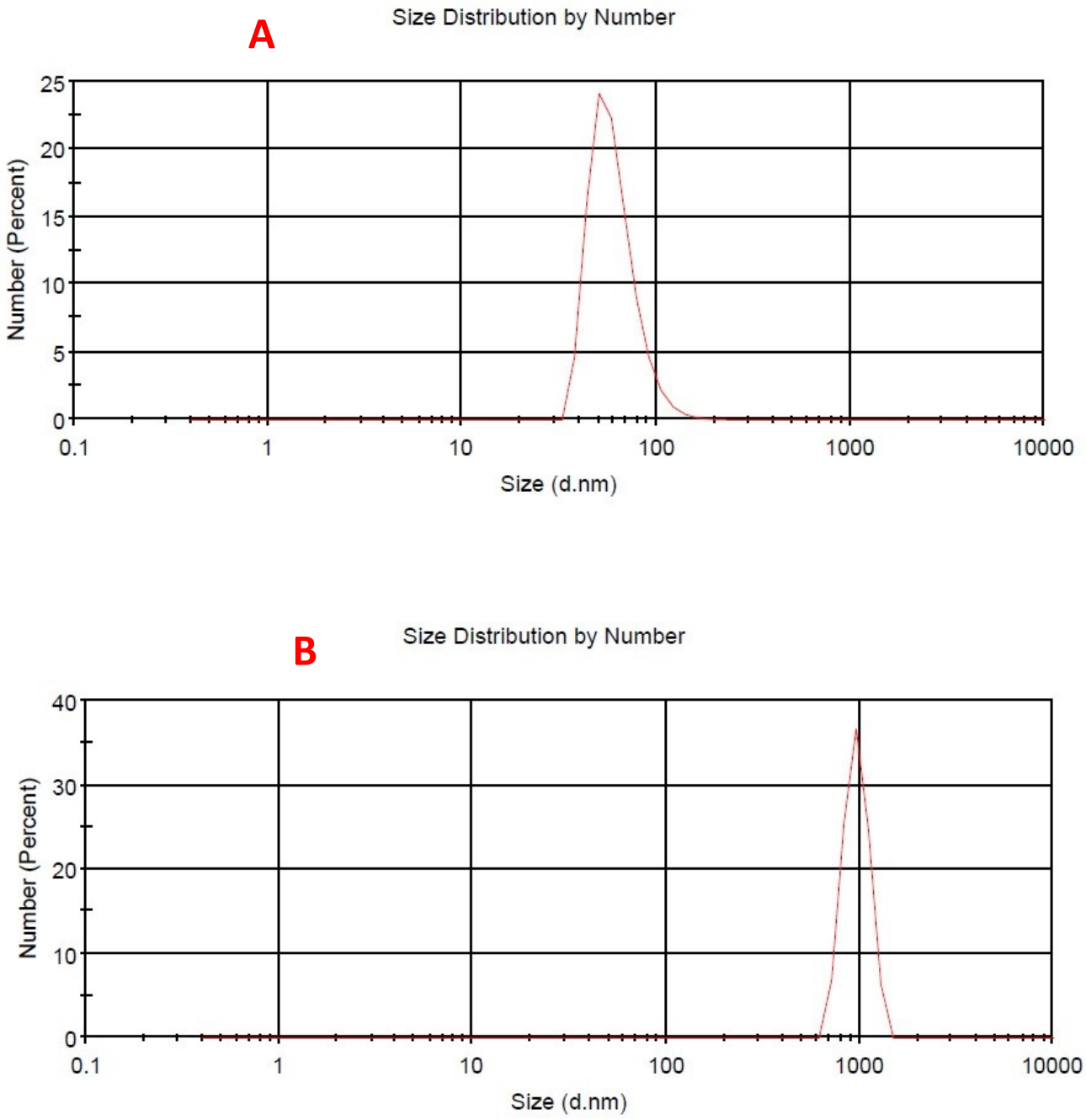

Figure S14. *Dynamic light scattering (DLS) analysis of* ***A)*** *Au@Ag core-shell NPs,* ***B)*** *Au@Ag core-shell NPs and uric acid mixture.*

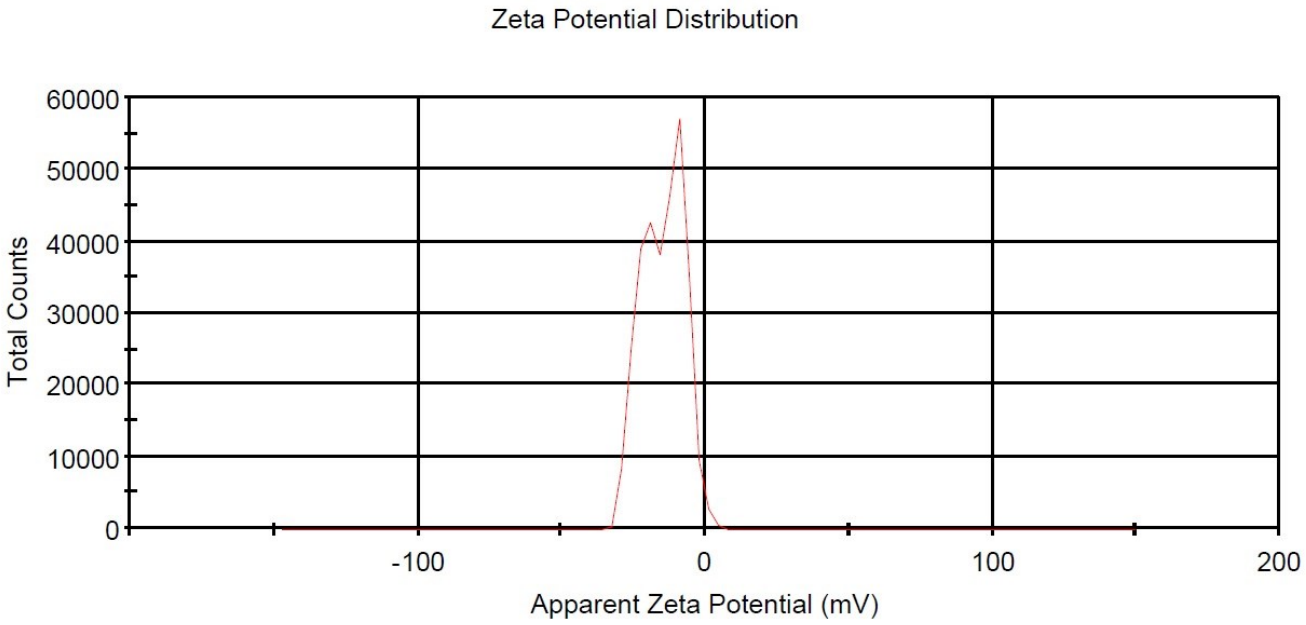

Figure S15. *Zeta potential of Au@Ag core-shell NPs.*

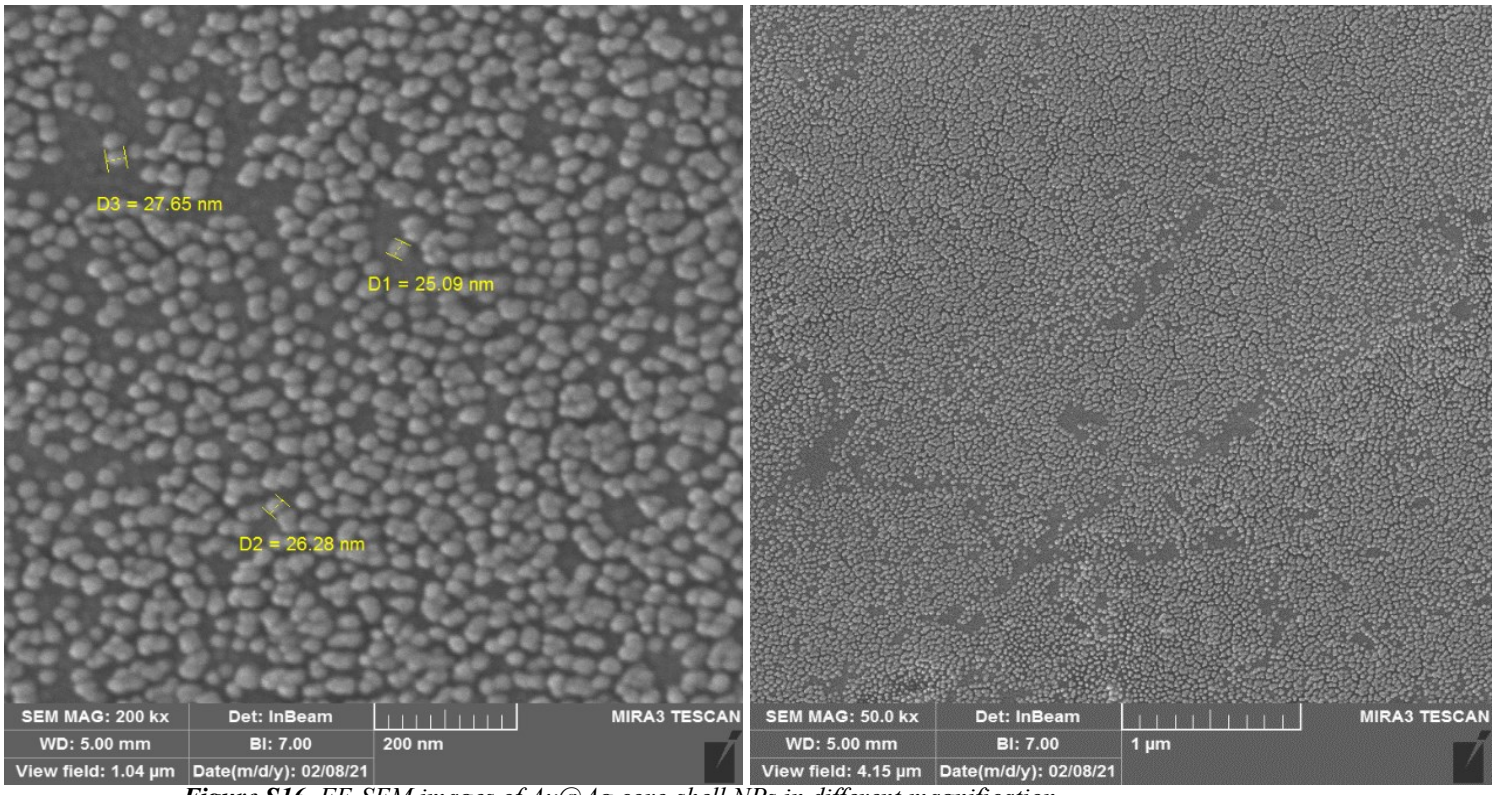

Figure S16. *FE-SEM images of Au@Ag core-shell NPs in different magnification.*

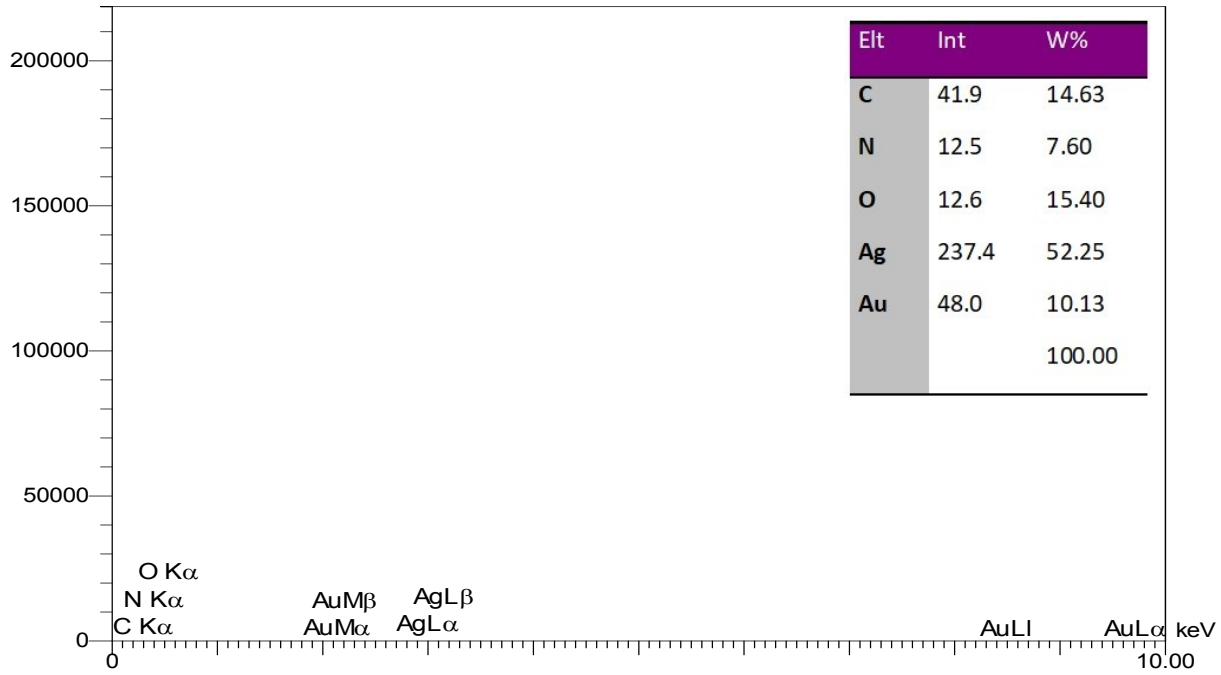

Figure S17. *EDS spectra of Au@Ag core-shell NPs.*

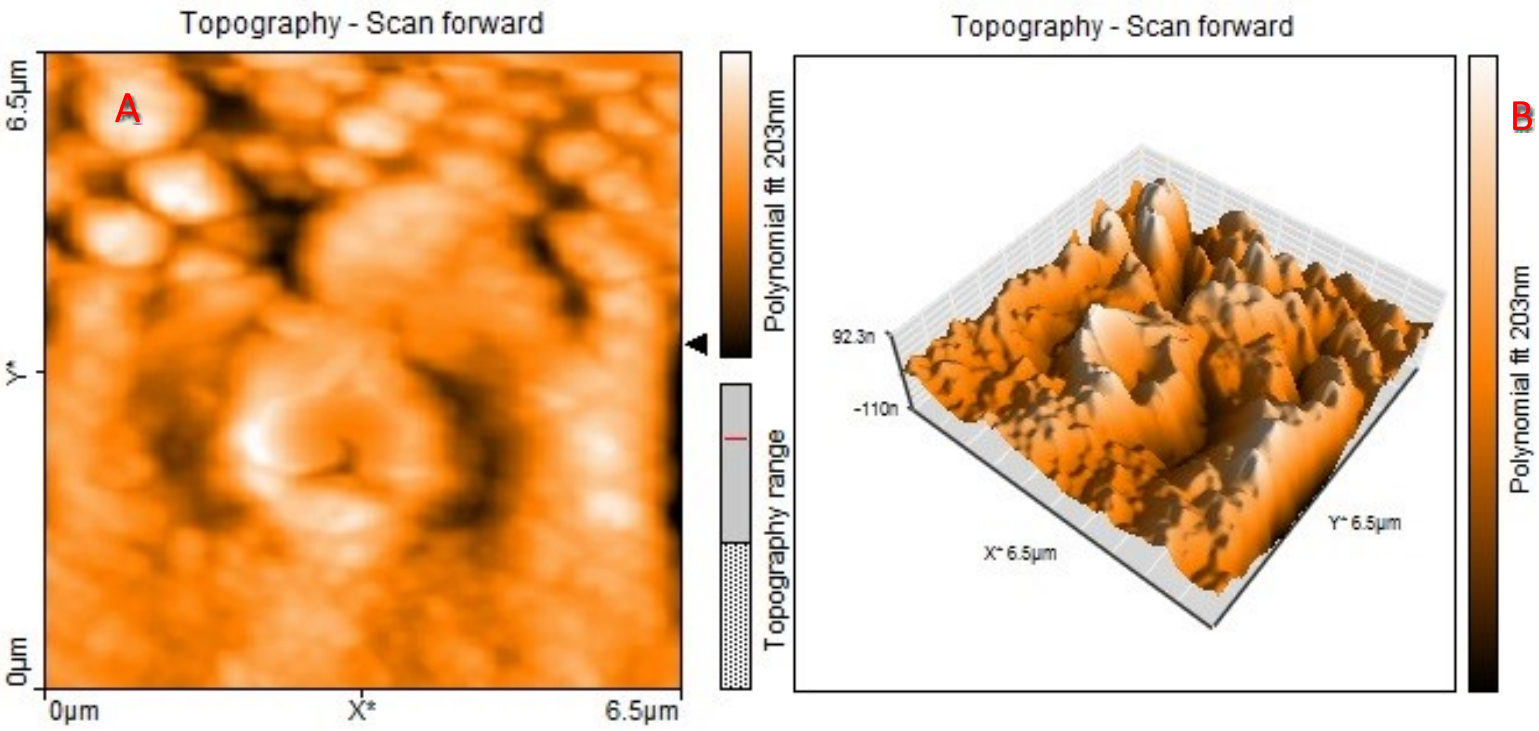

Figure S18. *Topographic AFM images in 2D* ***(A)*** *and 3D* ***(B)*** *view of Au@Ag core-shell NPs.*

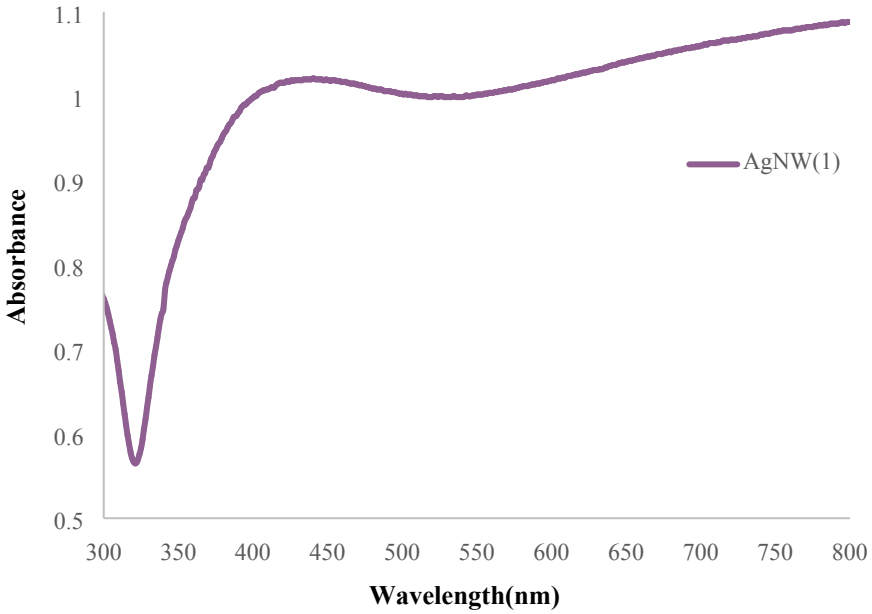

Figure S19. *UV-Vis absorbance spectrum of Ag NWs.*

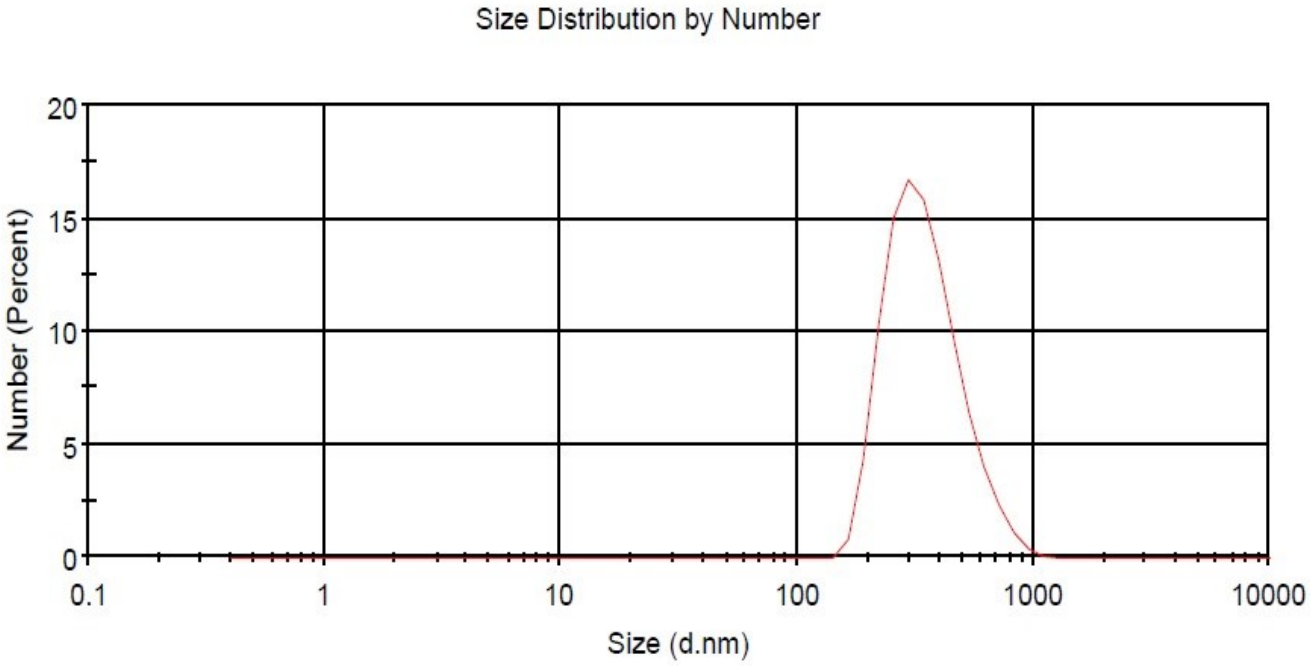

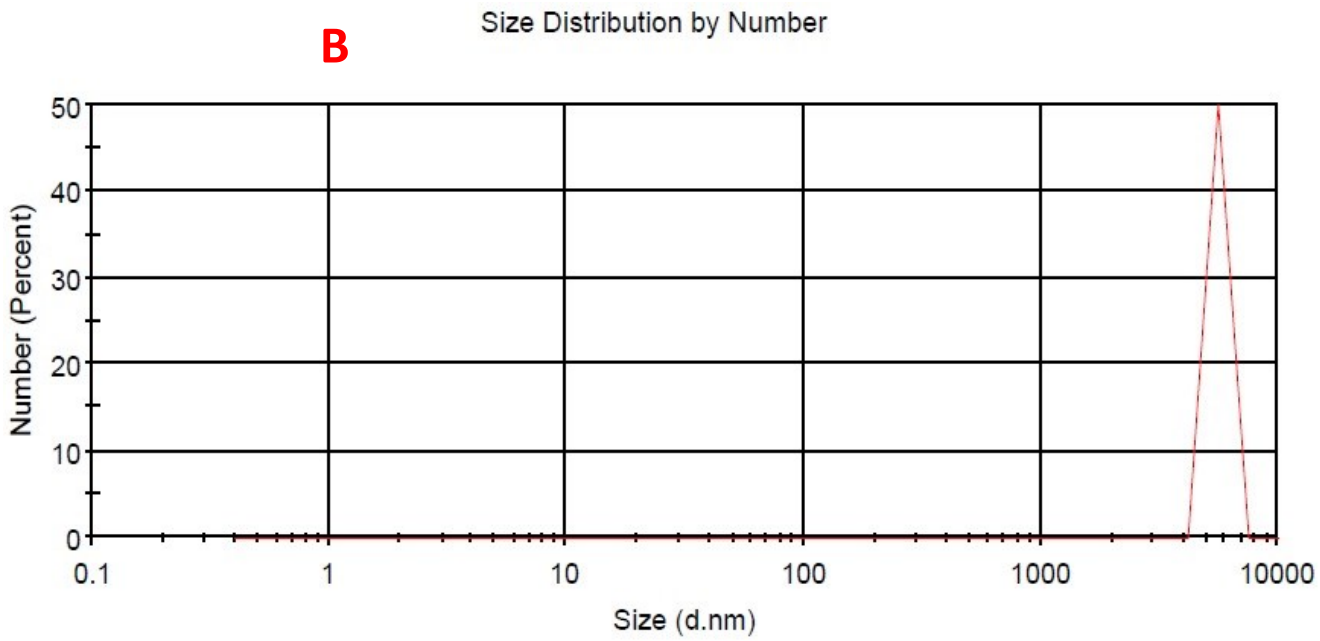

Figure S20. *Dynamic light scattering (DLS) analysis of* ***A)*** *Ag NWs,* ***B)*** *Ag NWs and uric acid mixture.*

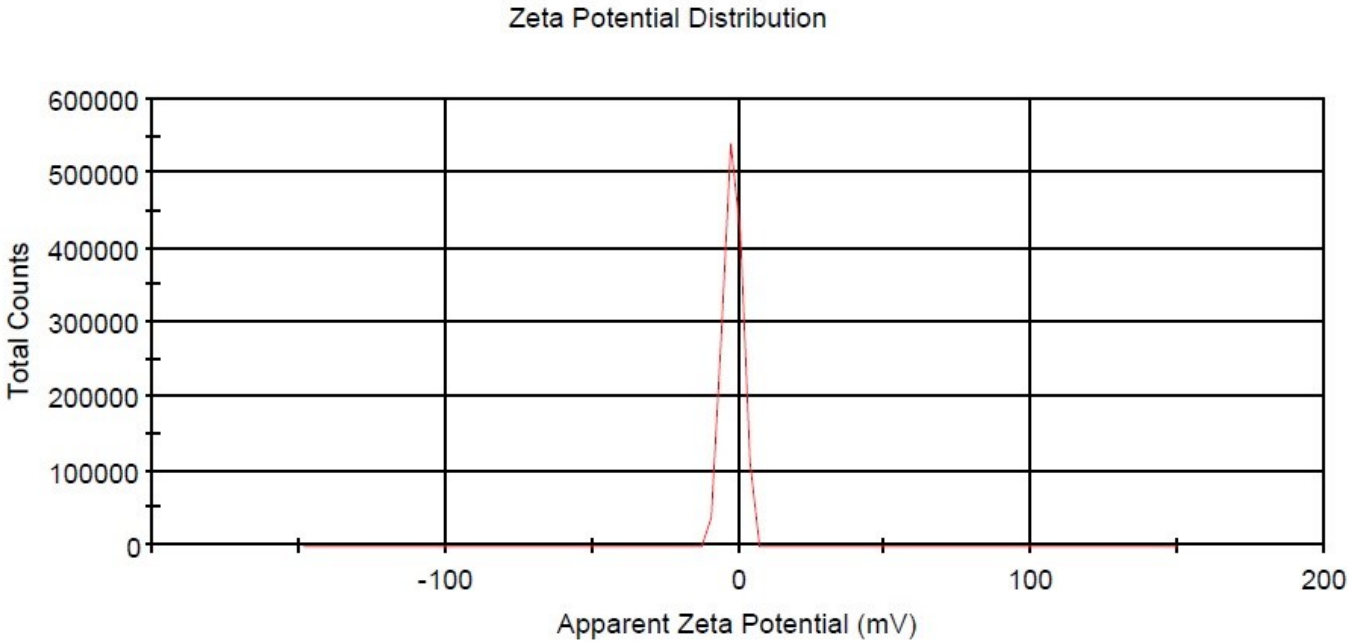

Figure S21. *Zeta potential of Ag NWs.*

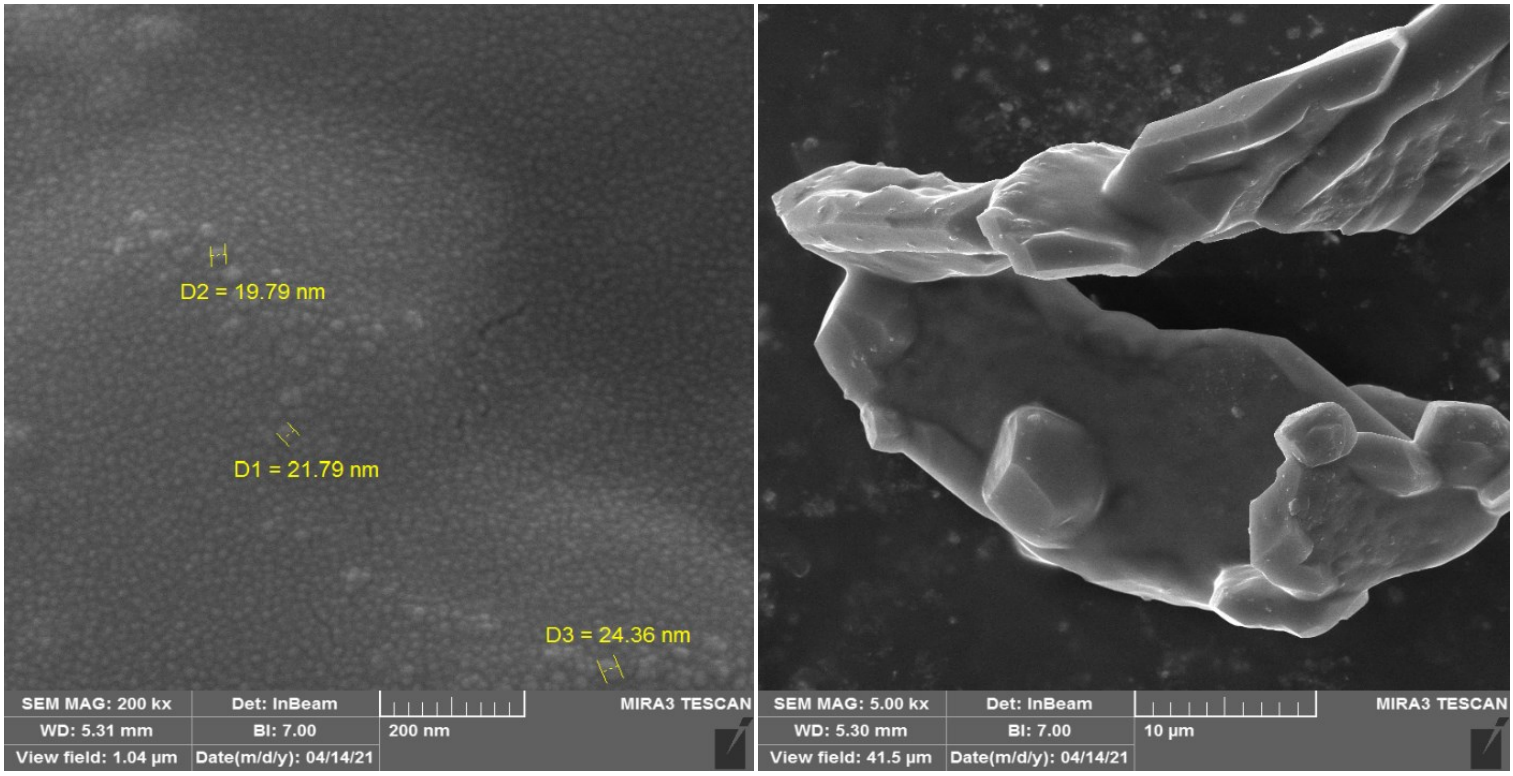

Figure S22. *FE-SEM images of Ag NWs in different magnification.*

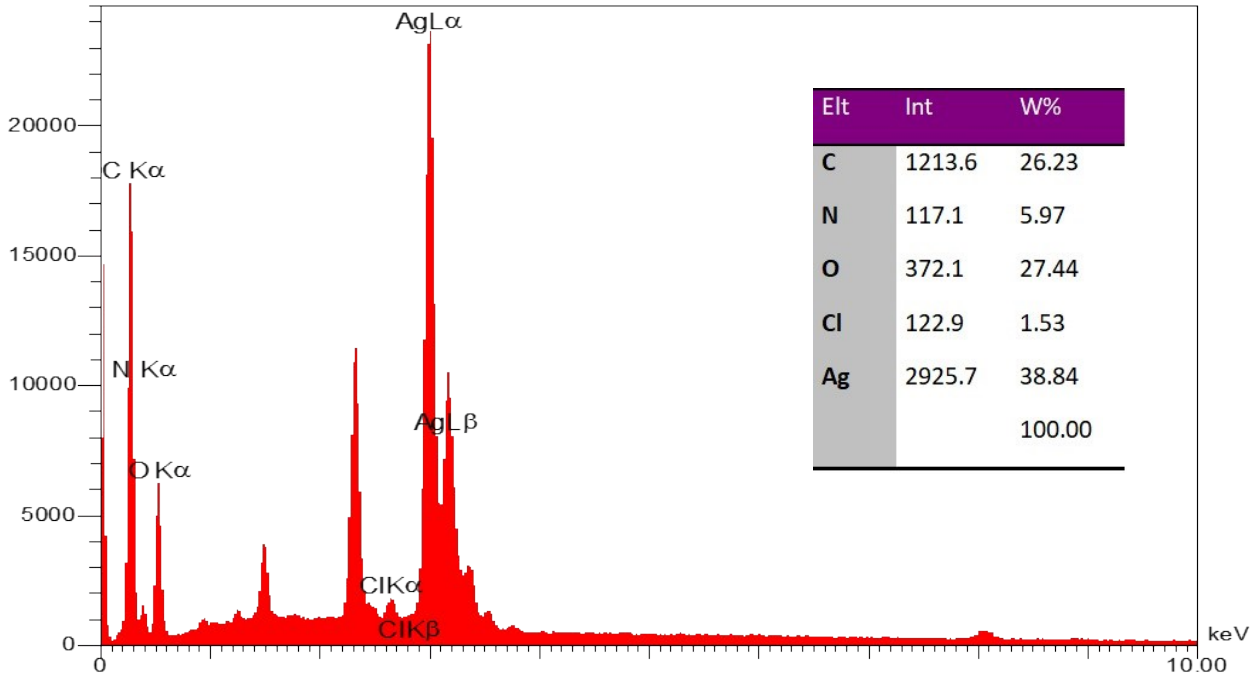

Figure S23. *EDS spectra of Ag NWs.*

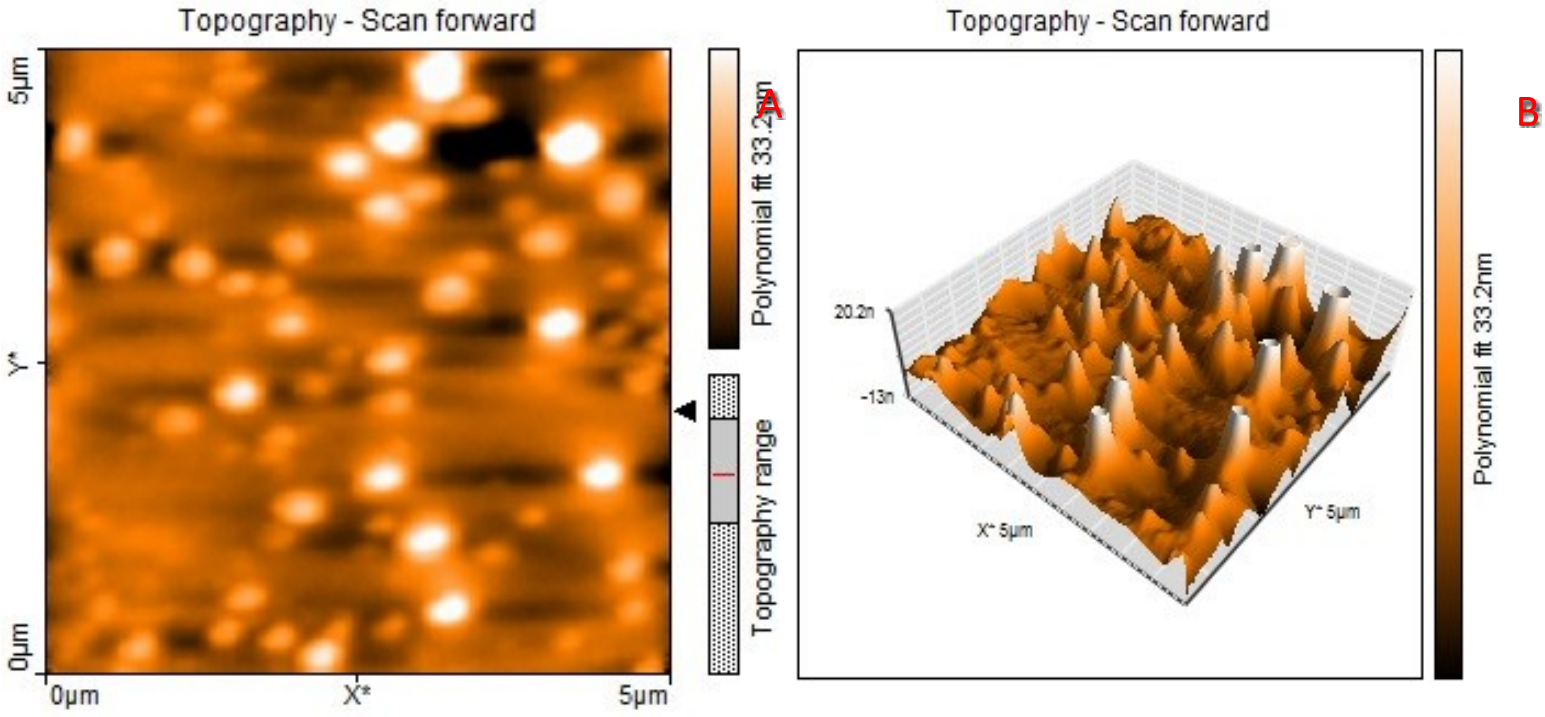

Figure S24. *Topographic AFM images in 2D* ***(A)*** *and 3D* ***(B)*** *view of Ag NWs.*

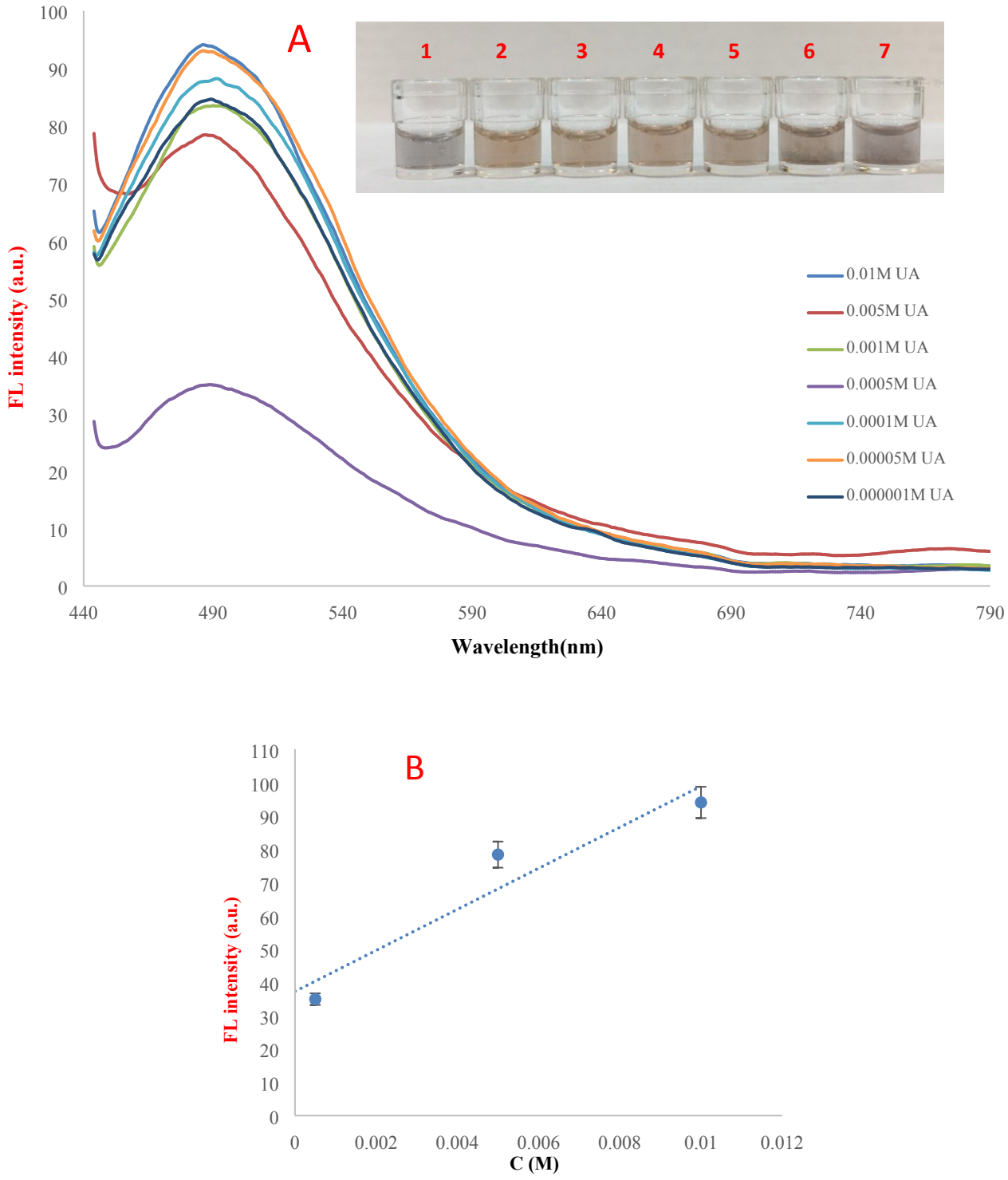

Figure S25. A) *Digital image and UV-Vis spectra recorded from reaction systems containing Ag citrate NPs, (TMB+H_2O_2+Met) and different concentration of UA (0.01, 0.005, 0.001, 0.0005, 0.0001, 0.00005 and 0.00001 M),* ***B)*** *Calibration curve of peak intensity versus concentration of UA.*

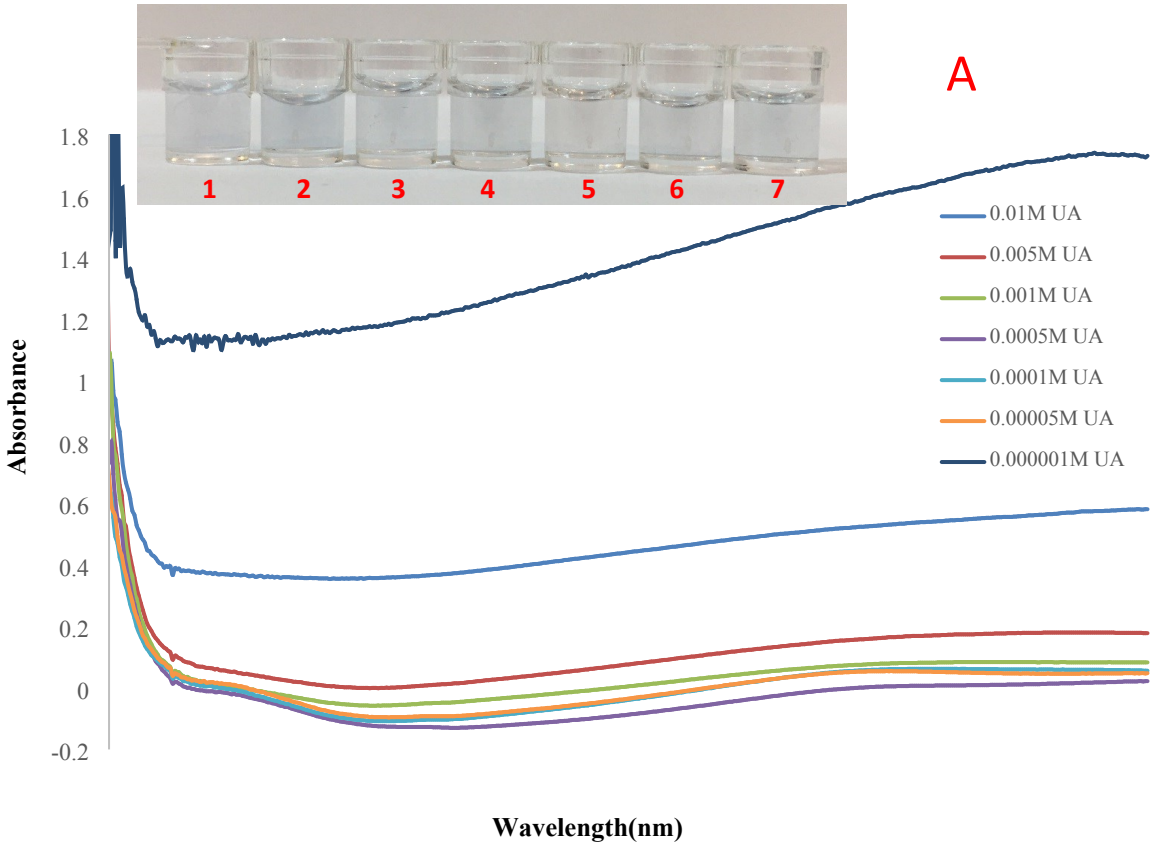

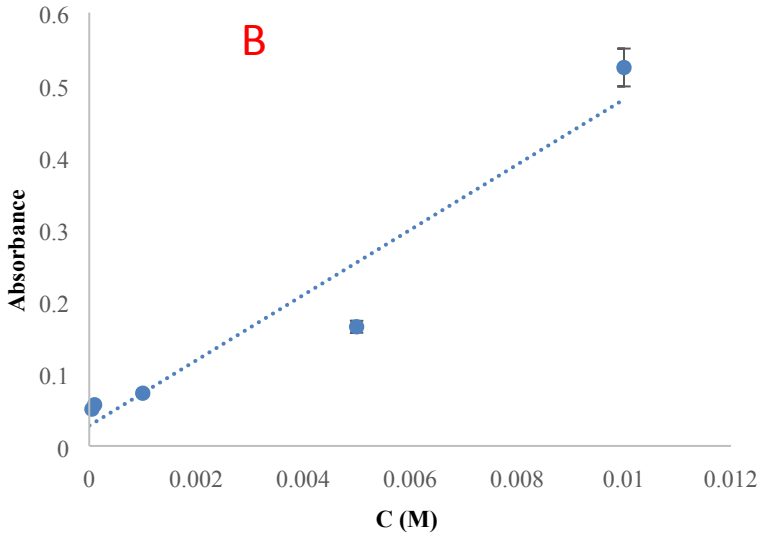

Figure S26. A) *Digital image and UV-Vis spectra recorded from reaction systems containing Ag NPrs, (TMB+H_2O_2+Met) and different concentration of UA (0.01, 0.005, 0.001, 0.0005, 0.0001, 0.00005 and 0.00001 M),* ***B)*** *Calibration curve of peak intensity versus concentration of UA.*

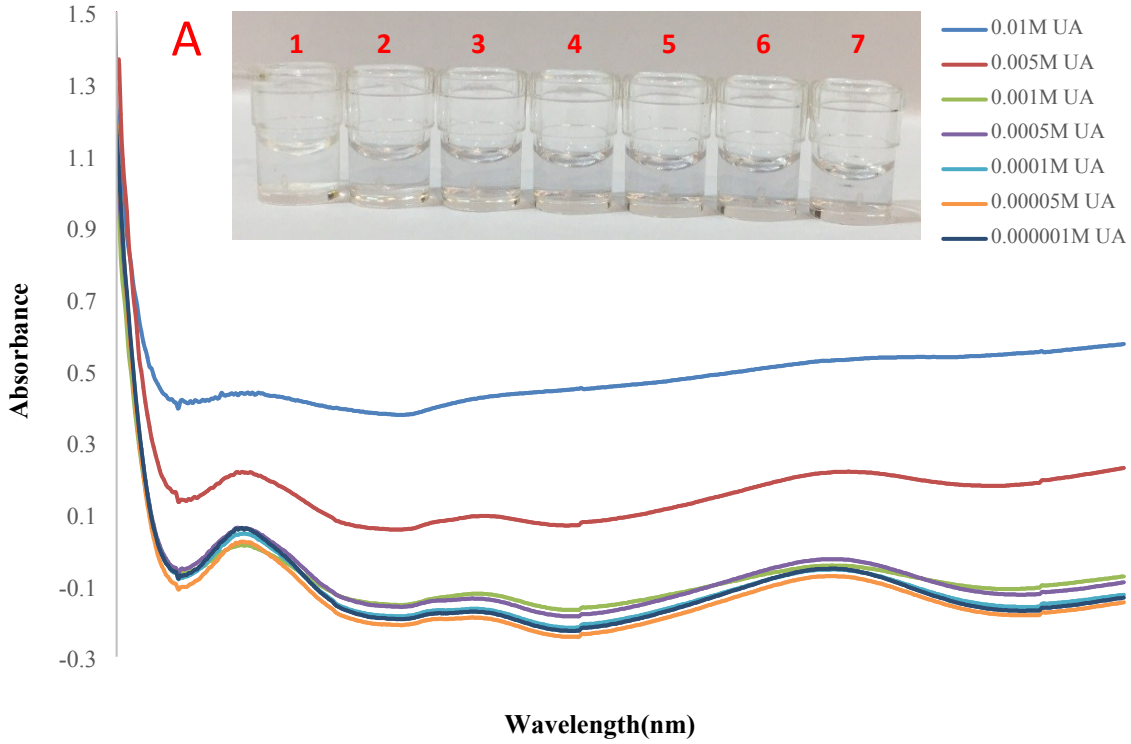

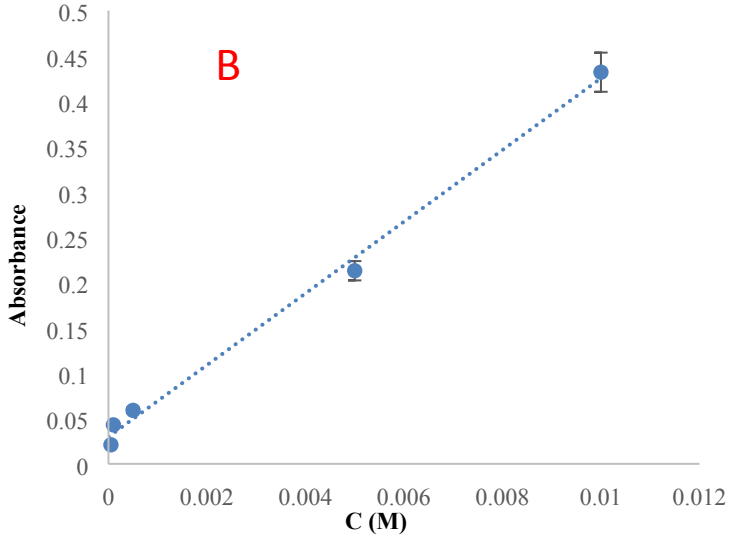

Figure S27. A) *Digital image and UV-Vis spectra recorded from reaction systems containing Au@Ag core-shell NPs, (TMB+H_2O_2+Met) and different concentration of UA (0.01, 0.005, 0.001, 0.0005, 0.0001, 0.00005 and 0.00001 M),* ***B)*** *Calibration curve of peak intensity versus concentration of UA.*

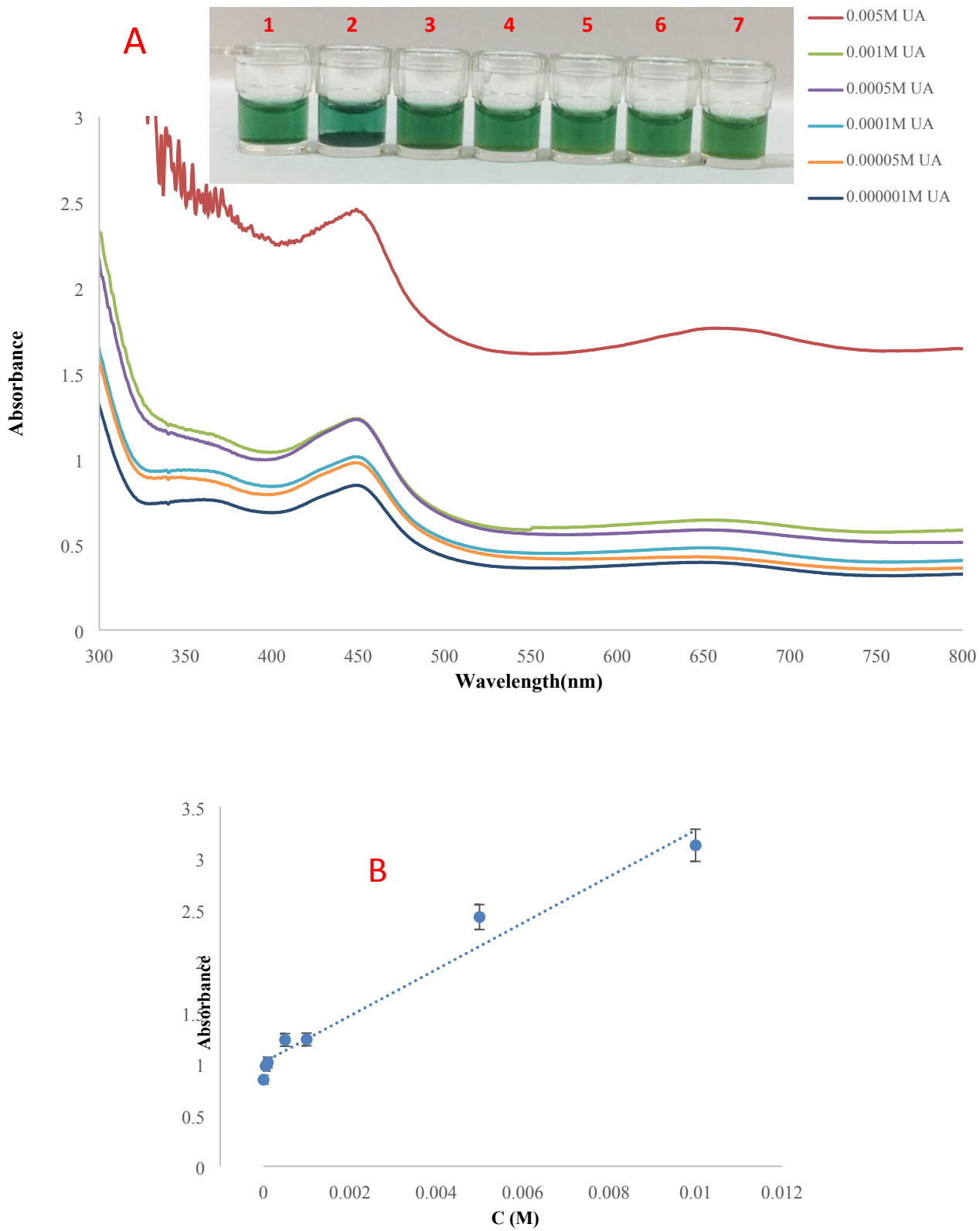

Figure S28. A) *Digital image and UV-Vis spectra recorded from reaction systems containing Ag NWs, (TMB+H_2O_2+Met) and different concentration of UA (0.01, 0.005, 0.001, 0.0005, 0.0001, 0.00005 and 0.00001 M),* ***B)*** *Calibration curve of peak intensity versus concentration of UA.*

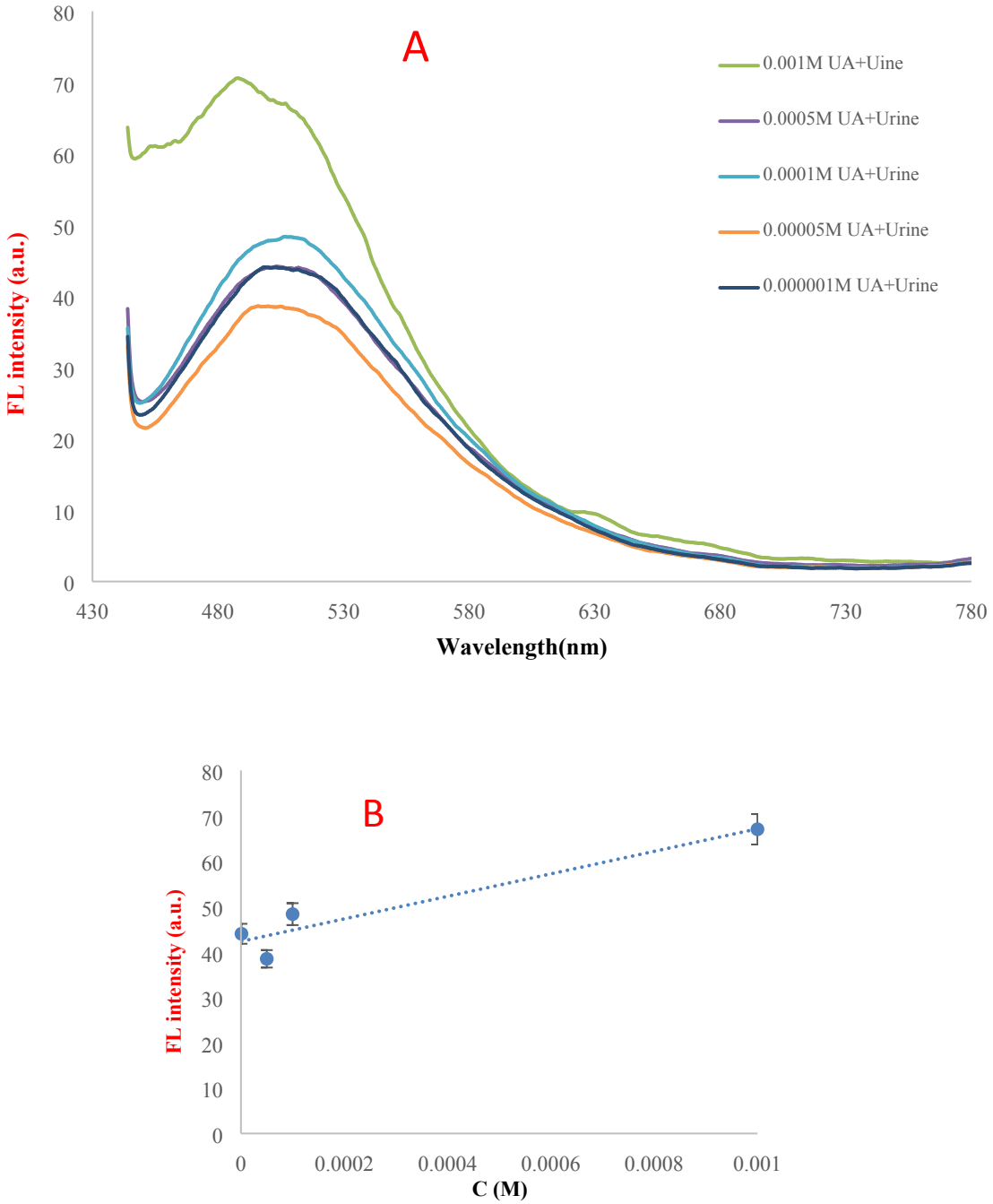

Figure S29. A) *Emission response for uric acid with increasing concentrations (0.00001, 0.00005, 0.0001, 0.0005, and 0.001 M) and Ag citrate in human urine specimens,* ***B)*** *Calibration plot of peak intensity versus concentration of UA.*

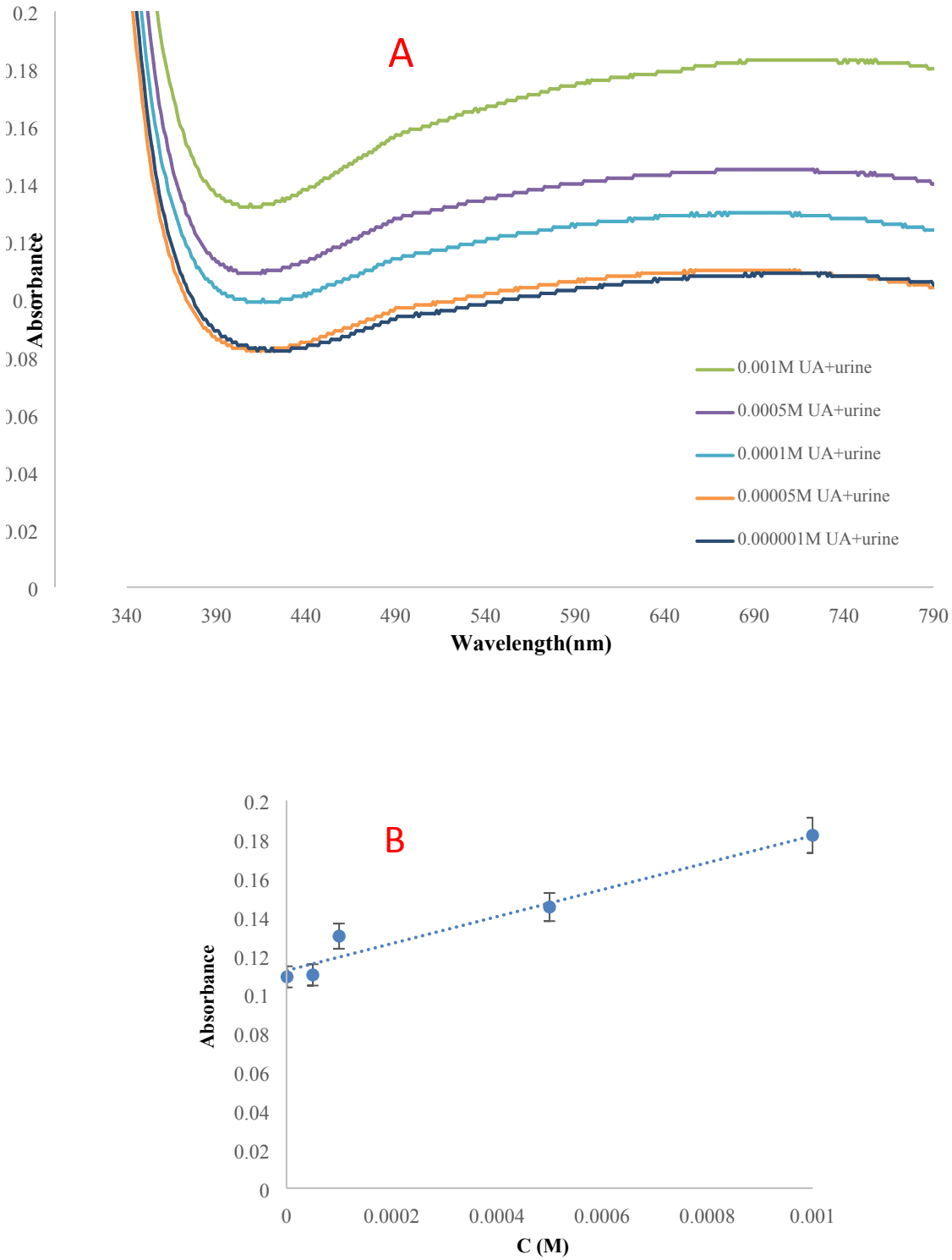

Figure S30. A) *Absorption response for uric acid with increasing concentrations (0.00001, 0.00005, 0.0001, 0.0005, and 0.001 M) and Ag NPrs in human urine specimens,* ***B)*** *Calibration plot of peak intensity versus concentration of UA.*

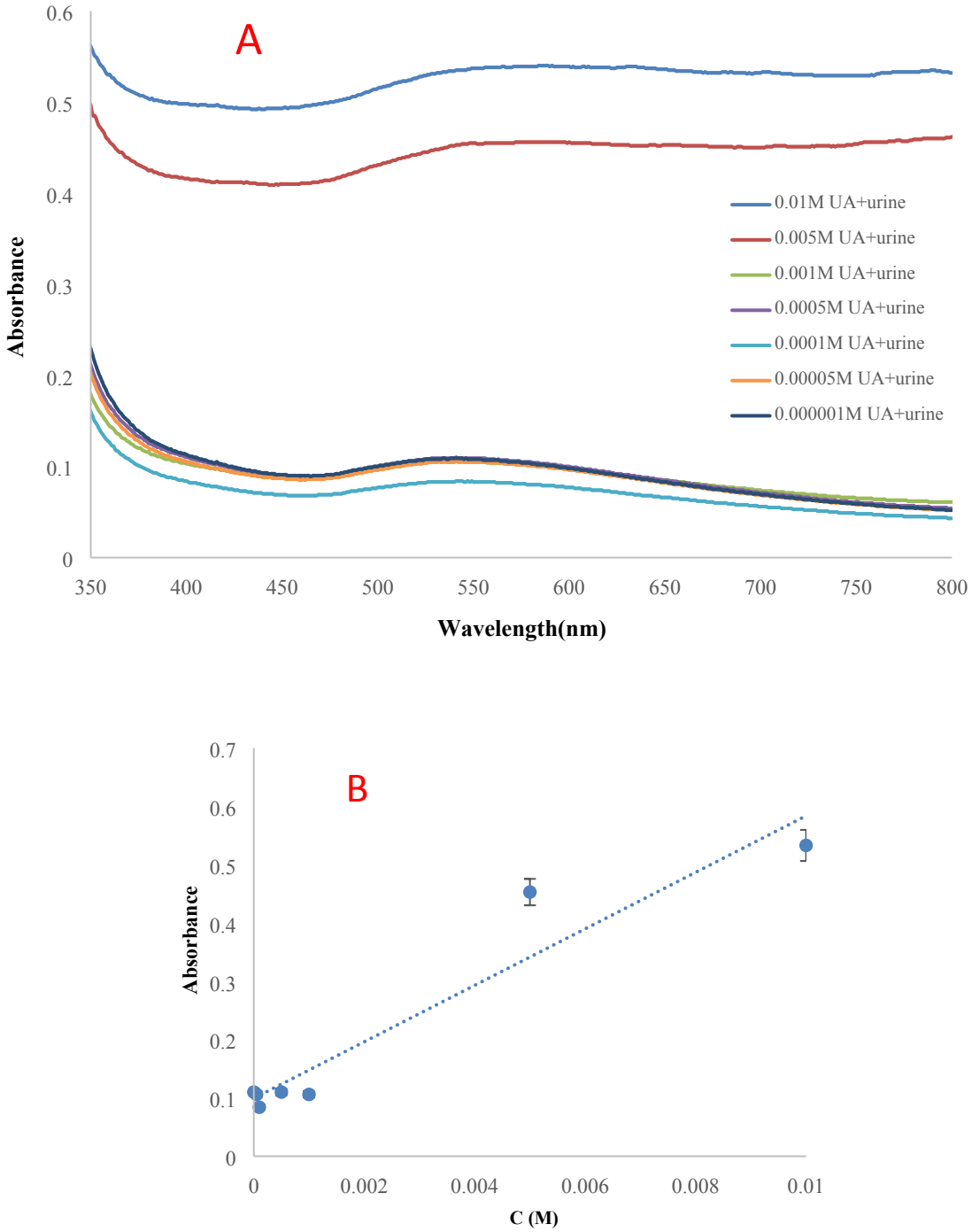

Figure S31. ***A)*** *Absorption response for uric acid with increasing concentrations (0.00001, 0.00005, 0.0001, 0.0005, 0.001, 0.005, and 0.01 M) and Au@Ag core-shell NPs in human urine specimens,* ***B)*** *Calibration plot of peak intensity versus concentration of UA.*

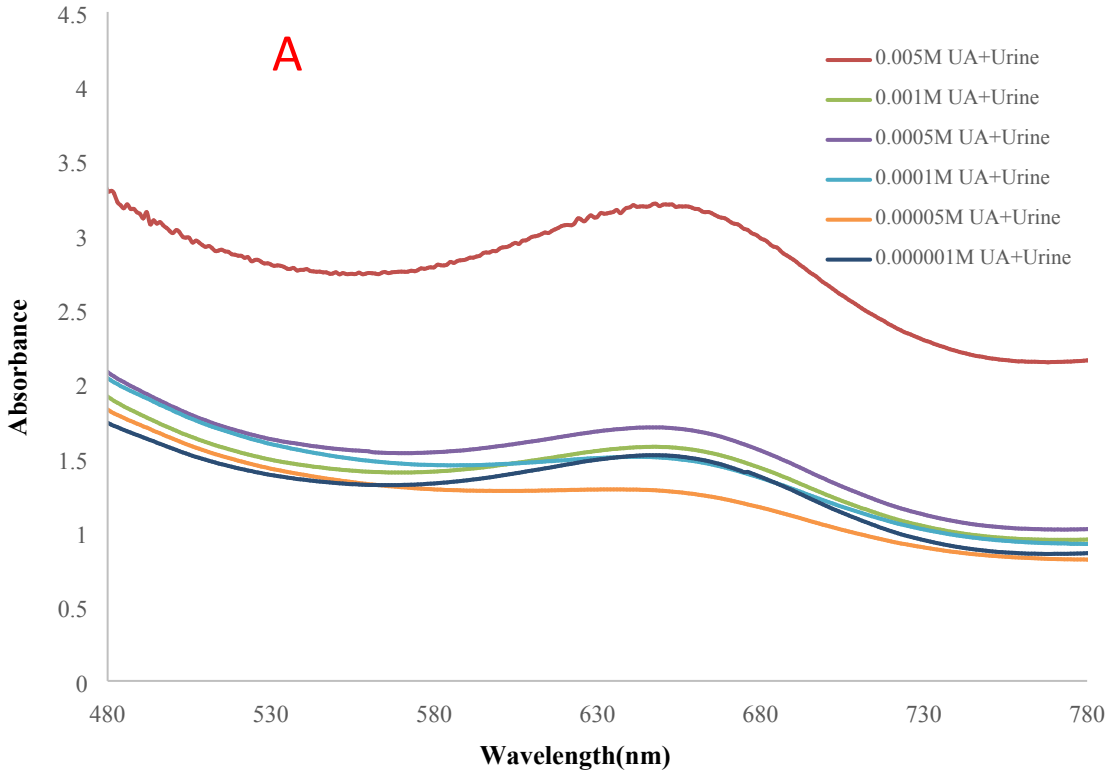

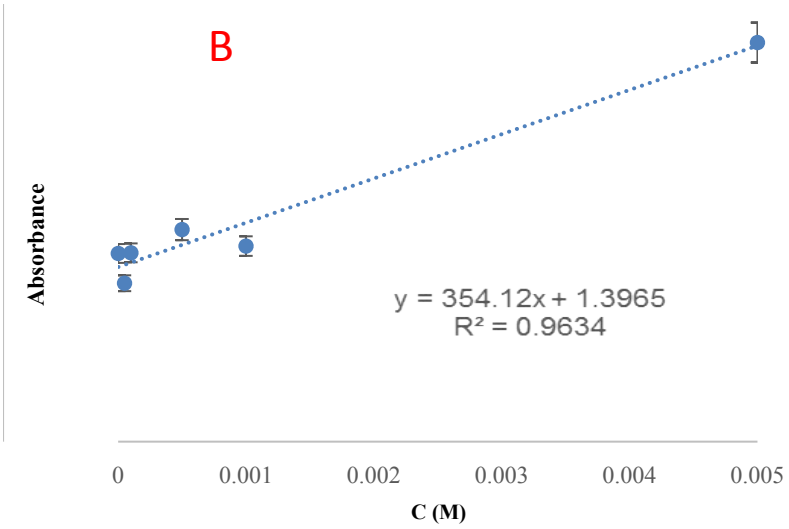

Figure S32. A) *Absorption response for uric acid with increasing concentrations (0.00001, 0.00005, 0.0001, 0.0005, 0.001, and 0.005 M) and Ag NWs in human urine specimens,* ***B)*** *Calibration plot of peak intensity versus concentration of UA.*